CHALMERS

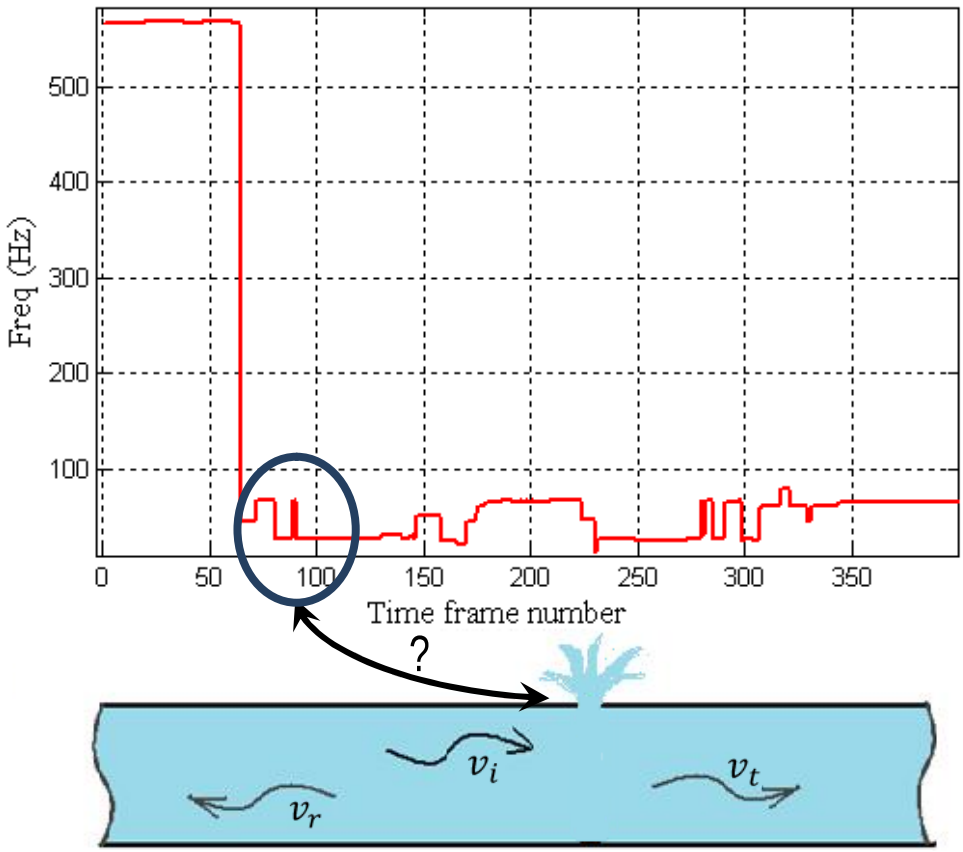


# Leak detection in plastic water pipe using pulse-echo method

Master's Thesis in the Master's programme in Sound and Vibration

SEYYED REZA HAQSHENAS

Department of Civil and Environmental Engineering
*Division of Division of Applied Acoustics*
*Vibroacoustics Group*
CHALMERS UNIVERSITY OF TECHNOLOGY
Göteborg, Sweden 2010
Master's Thesis 2010:128

MASTER'S THESIS 2010:128

# Leak detection in plastic water pipe using pulse-echo method

Master's Thesis in the Master's programme in Sound and Vibration

SEYYED REZA HAQSHENAS

Department of Civil and Environmental Engineering
Division of Division of Applied Acoustics
Vibroacoustics Group
CHALMERS UNIVERSITY OF TECHNOLOGY
Göteborg, Sweden 2010

Leak detection in plastic water pipe using pulse-echo method
Master's Thesis in the Master's programme in Sound and Vibration
SEYYED REZA HAQSHENAS



Master's Thesis 2010:128
Department of Civil and Environmental Engineering
Division of Division of Applied Acoustics
Vibroacoustics Group
Chalmers University of Technology
SE-412 96 Göteborg
Sweden
Telephone: + 46 (0)31-772 1000

Leak detection in plastic water pipe using pulse-echo method
Master's Thesis in the Master's programme in Sound and Vibration
SEYYED REZA HAQSHENAS
Department of Civil and Environmental Engineering
Division of Division of Applied Acoustics
Vibroacoustics Group
Chalmers University of Technology

ABSTRACT

This research project was proposed and supported by Ultrac AB company dealing with acoustical monitoring of leaks in buried water distribution pipes. The basic principle is the fact that water spouting out of a leak in a pressurized pipe generates acoustic noise, and this noise contains information as to whether a leak exists and hopefully of where it is located.

Acoustic methods for finding leaks are mainly based upon correlation analysis, where one sensing device is installed at each side of a leak. The two received acoustic signals are correlated and the arrival time difference represents a measure of the leak position. Theoretically, this can provide very high precision for metallic pipes. The main drawback is lack of generality. The correlation techniques nearly always fail to yield a precise prediction when applied on plastic pipes.

This study consists of applying and evaluating pulse-echo method for pinpointing leaks. This technique has been used in diagnosis of power lines for many years. The main concept is to send out a known burst and analyze the received signal to detect tracks of leakage. One expects to observe Doppler shift in modulated signal wave due to dynamic disturbances in water pipe in vicinity of leaking point caused by escaping water. This report starts with the introduction section to outline an overview of leak detection problem. It continues with the theory section that explains a model for prediction of sound field as a result of reflection of reference acoustic wave from a moving reflector. The experimental part involves applying this technique in urban water pipeline system and measurements results. Subsequently signal processing section covers analysis of data and final results. Eventually this work is summarized in conclusion and summary section.

Key words: Leak detection, Water pipeline, Pulse-echo, Doppler shift, Time-Frequency analysis, Maximum Likelihood Estimator (MLE)

# Acknowledgement

In this study, the idea of leak detection in plastic water pipe with the aid of pulse-echo technique has been evaluated theoretically and experimentally. All the experiments have been carried out on Göteborg urban pipeline system at Stenkolsgatan between March 2010 to July 2010. The project is carried out at the Division of Applied Acoustics, Chalmers University of Technology, Sweden and financially supported by ULTRAC AB.

I would like to offer my sincerest gratitude to my supervisor, Professor Wolfgang Kropp, who has supported me throughout my thesis with his knowledge and smart ideas. The practical part of this work would not have been possible without kind and skilful supports from Börje Wijk. I would also like to thank ULTRAC AB and specially Gösta Lange for their close co-operation and procurement of transducers.

Last but not the least, I would like to extend my gratitude and acknowledgements to my family for their incredible love, support and encouragements. I certainly owe my progress to them. Love you.

Göteborg August 2010

Seyyed Reza Haqshenas

# Contents

# 1 Introduction to leak detection

The problem of leaks in underground water pipeline has been source of concerns for a long time due to its potential danger to public health, economic loss, environmental damage and wastage of energy. In dry parts of the world, e.g. Middle East, drinking water is a precious commodity and monitoring hydraulic network to save water is significantly important.

An unintended hole, crack, or the like, through which liquid, gas, light, etc., enters or escapes is called leak. In piping, Leaks include those from service connections, a faulty joint, and a cracked pipe. The problem of leak detection can be classified as a subcategory of an important research field named Condition Monitoring. The objective, however, is not to predict indications of probable failure but it is to capture tracks of existing defect (crack) in the pipe.

One of the earliest leak detection works dates back to 1920 by Babbit [1] which attempted to pinpoint the leak by listening to the noise attributed from it in the pipeline. Exit of water from an opening on the pipe wall may cause several physical changes in the pipe and surrounding soil such as pressure drop in the pipe, making acoustic noise, changing moisture of soil and etc. Every of these phenomena can be used as a key symptom for monitoring water distribution network. Some of the widely used approaches were explained in the following but for more comprehensive overview of existing leak detection techniques for water pipeline please refer to Andrew , et. al. [2].

## 1.1 Ground penetrating radar

Radar generates an image based on reflection of radar waves from changing densities of soil/pipe. In fact it detects variation in bulk physical properties such as voiding or saturation of soil caused by leaked water. This technique suffers from some disadvantages, major ones are:

- Expensive equipments
- Hard to interpret especially for unmapped services (pipeline)
- Restricted operational range
- Significant operator training and experience

## 1.2 Infrared thermography

Infrared radiation detector locates temperature difference caused by the leaking liquid in near ambient conditions, see Inagaki et. al. [3]. This is a good method for restricted area or short superficial pipelines but sustains from disadvantages like:

- Expensive tool kit
- Significant operator training and experience
- Weather dependent
- Accurate only for near ambient conditions

## 1.3 Acoustic-based methods

This category includes all techniques that try to locate leakage with the aid of sound generated from it. Basic approaches are very simple, just by listening to either sound field in the pipe by placing hydrophone in direct contact with the pipe or its appurtenances, e.g. hydrants, or radiated sound to the ground by listening stick[1]. More complicated approaches diagnose pipe by capturing change in Frequency Response Function (FRF) of it because of the leak or by estimation of time delay between recorded signals with different sensors. The latter idea has been practically successful and therefore widely used for leak detection. Due to important role of this technique in leak detection of water supply networks it was explained more thoroughly in the following.

### 1.3.1 Time delay estimation for leak detection in buried water pipes

Briefly speaking, two sensors are placed on opposite sides, though not far away, of leak to hear leaking sound, then spectra of the recorded sounds are inputted to a computer (analyzer). Subsequently cross-correlation function of two spectra is calculated and results presented. In the Figure 1.1 a typical measurement arrangement and access points where sensors can be attached were depicted.

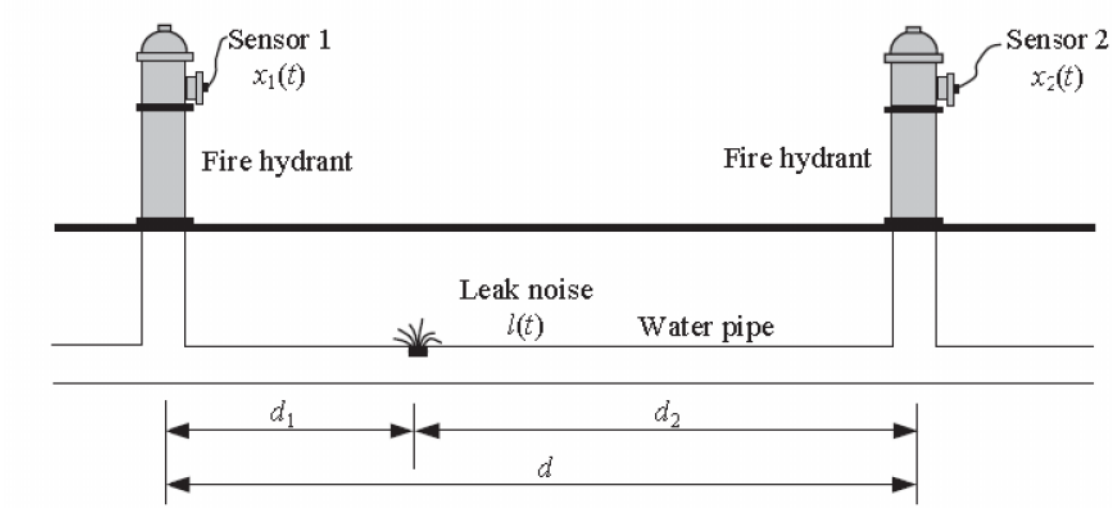


Figure 1.1: Schematic of leak point in buried pipe and access points [4].

d1 and d2: distances of each access point from leak, unknown

d: distance between access points (d= d1 + d2), known X1(t) and X2(t): measured signals by hydrophones or accelerometers, assumed to be stationary, continuous, random signals with zero mean values

Cross-correlation function is defined by

[1] Listening stick or listening rod is consisting of a single transducer at the end of a rod, amplifier and output device which can be a headphone or a simple amplitude meter.

$$R_{X_1X_2}(\tau) = E(X_1(t)X_2(t+\tau)) \tag{1.1}$$

where E() is expectation (mean value) operator. Cross-correlation function calculation is concisely illustrated in the Figure 1.2, Please refer to Gao et. al.[4] for extended information.

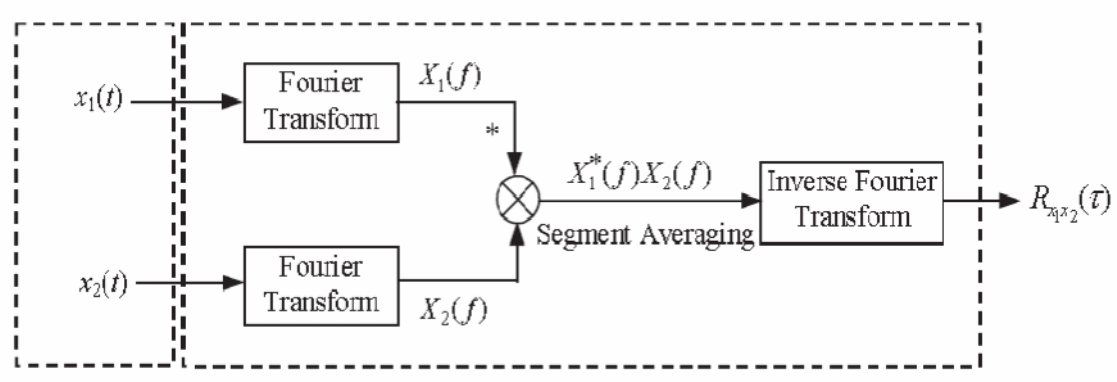


Figure 1.2: Schematic of the implementation of the basic cross-correlation function. $X_1$* is the complex conjugate of X1 [4]

The value of $\tau$ that maximizes $R_{X_1X_2}(\tau)$ ; denoted as $\tau_{peak}$ , provides an estimate of time delay between two signals. Since time delay is related to the position of sensors, knowing the wave speed in the pipe, the leak can be pinpointed using the following equations:

$$\tau_{peak} = \frac{d_1 - d_2}{c} \quad \Rightarrow \quad d_1 = \frac{d - c\tau_{peak}}{2} \tag{1.2}$$

Acoustic signals in plastic pipes are heavily attenuated and generally narrow-band and of low frequency [4]. The effectiveness of the correlation technique was found to be affected by several factors, including the selection of vibration sensors and cut-off frequencies of digital filters. Background noise level and signal to noise ratio (SNR) influence output of this technique considerably. The main pros are:

- Can find leaks that other acoustic methods are handicap
- Accurate
- Less depends on operator skills
- Easy to use

And main cons are:

- Contact location required
- Quiet leaks are hard to correlate
- Poor performance on PVC/large diameter pipes due to interfering signals from external sources and excessive signal attenuation

In the present research work, a new idea for detection of leak in buried plastic water pipes has been proposed and investigated theoretically and

experimentally. The essence of this idea is that water exiting from opening makes fluctuations and swirling motion in the flow inside pipe which should work as a moving reflector, therefore if an acoustic wave impinges upon this reflector (vicinity of leak) it would be reflected back but in a different frequency caused by Doppler shift phenomena. This study is amongst the first researches about this concept, no literature could be found that has already evaluated similar idea. Bimpas et. al. [5] applied similar procedure for leak detection of buried plastic pipes but he used continuous wave Doppler sensing by emitting electromagnetic waves (Not sonic waves) at frequency of 2.45 GHz (that study can be classified in a category of ground penetrating radar approaches). They could sense Doppler shift in the range of 1.6 mHz to 0.32 Hz for different leak sizes and flow rates [5]. That was published on March 2010.

Theory of Doppler was developed in the next section in order to predict effect of a moving reflector-with single and multiple-frequency harmonic motion on incident acoustic wave.

## 1.4 Wave propagation in water pipe

Before continuing to the next section some important points about wave propagation in pipes should be remarked here. The problem of acoustic wave propagation in a fluid-filled pipe has been subject of extensive research for a long time and it is not the intention of this section to represent them again here but just to point out to some important results of those researches. Interested reader is referred to works by professor Brennan at ISVR like [6], [7],[8]. Brennan .et. al [6] determined the wave speed in a 170mm MPDE plastic pipe theoretically and experimentally, shown in Figure 1.3. This graph confirms existence of dispersion in pipe which should be noted in our future analysis. Another significant point is high frequency-dependent damping in soft pipes. The higher the frequency the greater the energy dissipation per length is. This fact was approved both theoretically and experimentally by Brennan et. al [6] . Respecting results of all researches have been gone over and our own measurements data, the leak noise spectrum is narrow band and only has low frequency contents approximately below 150Hz.

According to data sheet pertinent to PEH pipes received from ULTRAC AB and brought in the Appendix A the wave speed in the piece of pipe used for outdoor measurements should be in the range of 250-450 m/s.

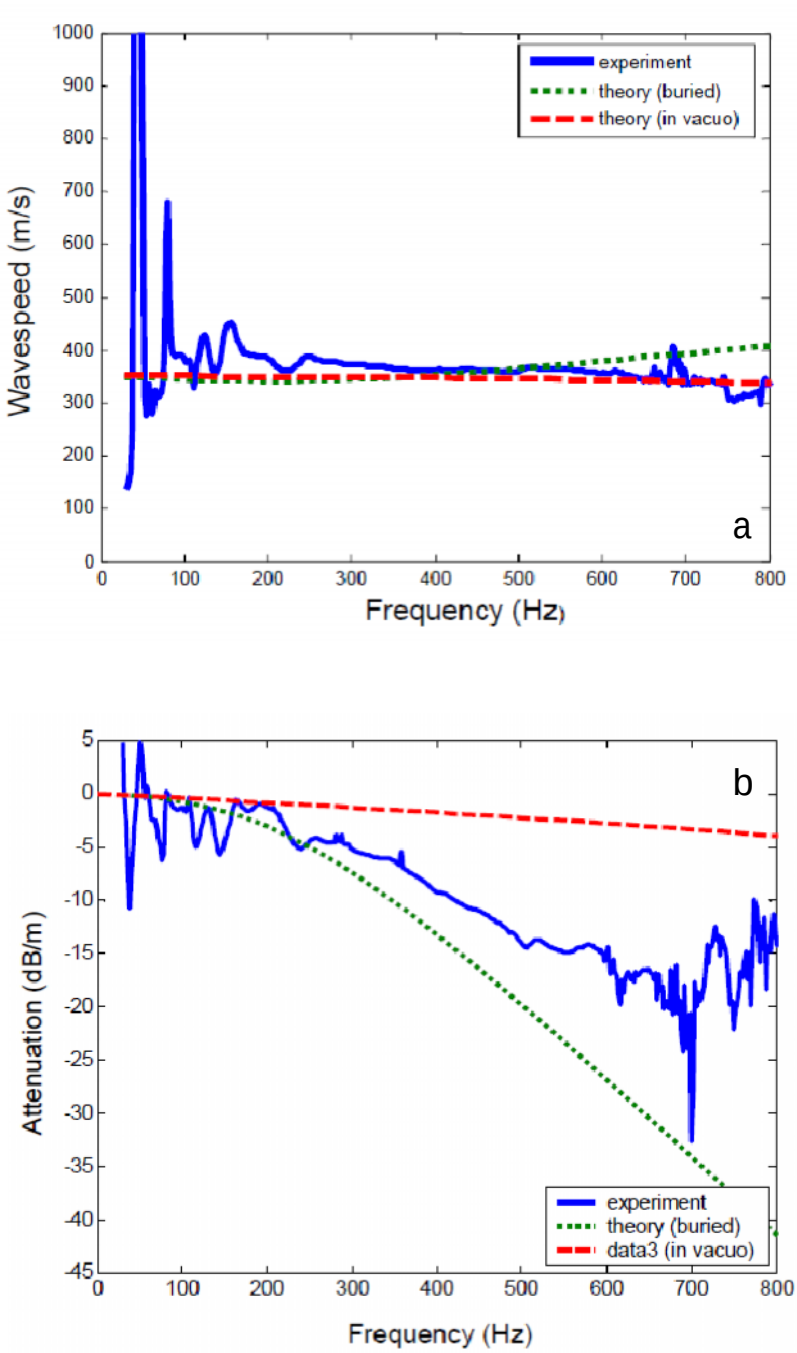


Figure 1.3: (a) Measured and predicted wave speed and (b) attenuation in a buried fluid-filled- plastic pipe

# 2 The Doppler shift theory

In this study, pipes of urban water distribution network were used for analysis. The pipe material for water supply network is usually PVC/ PE (polyethylene)/PEH (polyethylene high density) and in a inside diameter range of 15-19 mm. The pressure inside pipe provided by pumps in water facilities (upstream) is around 5 bar. Opening in the pipe wall causes a pressure gradient between the states inside and outside of the pipe and consequently fluid spouts out of the pipe. If this sudden change in pressure and therefore flow momentum is comparable with the upstream flow momentum it distorts the flow streamlines and lead to swirling motion in the vicinity of leakage. This can be explained as the vortex shedding phenomena. The flow regime in pipe is usually turbulent. The Reynolds number is determined with the formula (2.1). For a 16.6cm diameter pipe which encloses flowing water with an almost 1.3 m/sec discharge rate the Reynolds number is 213059. This high Reynolds number demonstrates turbulent flow inside the pipe.

$$Re = \frac{UD}{\nu} \tag{2.1}$$

U is the flow speed in pipe in m/sec, D is the pipe diameter in meter and $\nu$ is the kinematic viscosity of flow which for water is 1E-6 $m^2/s$.

This dynamic characteristic of flow is the essence of our proposed technique for leak detection. This discontinuity of flow in the pipe reflects acoustic energy sent to the pipe back but with a different frequency from its original one. Because of the whirling motion of flow and eddies are expected to be formed around the leak location the incident acoustic wave impinges on moving reflector. The sound wave generated due to the leakage discontinuity, i.e. the reflection, is therefore distorted from the incident wave because of relative motion between source (moving reflector) and observer. Source motion has a considerable effect on the generation of sound. The mono frequency tone radiated by a moving source with a linear translational motion is heard by the observer at the Doppler shifted frequency whereas periodic motion of the source creates new harmonics in the radiated wave, so observer hears a wave comprised of several tones. This unique feature of reflected sound discriminates it from other reflections caused by other discontinuities in the pipe like bendings, branches, etc. The aim of this chapter is to develop a mathematical model in order to predict the sound field from a moving source with harmonic motion. The procedure and results can be safely extended to a case where reflector oscillates with a multiple frequencies periodic motion.

## 2.1 The sound field of moving reflector (source) with harmonic motion in a pipe

This particular moving source was modelled as an oscillating piston presumed to be placed inside pipe (likely at the leak position). The piston face velocity at the moment t is $v_p(t)$ and its position therefore $x_p(t)$. A tone with frequency $\omega$ is sent out in the pipe as incident wave (reference signal). Schematic of pipe and moving piston were shown in Figure 2. 1.

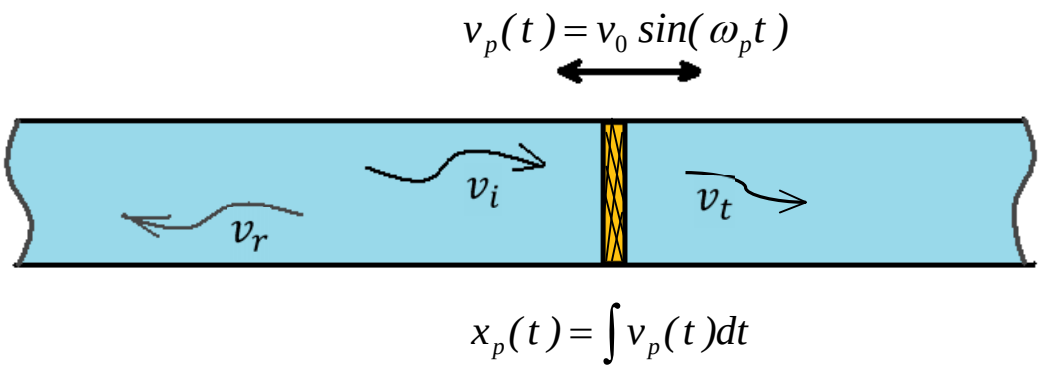


Figure 2. 2: Schematic of pipe with a harmonically oscillating piston in the leak spot

The sound field of a moving point source $(q(X,t) = Q(t)\delta(X - X_p(t)))$ can be obtained from the following relation [9]:

$$p(X,t) = \int_{-\infty}^{\infty} \frac{Q(\tau)\delta(t - \tau - |X - X_p(\tau)|/c)}{4\pi|X - X_p(\tau)|} d\tau \qquad (2.2)$$

Where X is position vector in the Cartesian coordinate system. $q(X,t)$ is a monopole point source with $Q(t)$ as the source strength. c is wave speed in the medium. $\delta(\tau)$ refers to Dirac delta function which is one at $\tau = 0$ and zero elsewhere. For the plane wave propagation in ducts the wave attenuation by distance is replaced by one. Thus the relationship (2.2) is reformulated to equation (2.3).

$$p(X,t) = \int_{-\infty}^{\infty} \frac{Q(\tau)\delta(t - \tau - |X - X_p(\tau)|/c)}{1} d\tau \qquad (2.3)$$

$p(X,t)$ defines the pressure field in the pipe at position X and instant t. In order to calculate above integral, It is necessary to find zeros of Dirac delta function, i.e. values of $\tau$ that satisfy the equation:

$$t - \tau - \frac{|X - X_p(\tau)|}{c} = 0 \qquad (2.4)$$

at each time instant t.

In our case, assuming a harmonic motion for the piston the equation (2.4) is written as:

$$X_p(t) = A_p \sin(\omega_p t) \tag{2.5}$$

$$t - \tau - \frac{\left| X - A_p \sin(\omega_p \tau) \right|}{c} = 0 \tag{2.6}$$

Values of $\tau$ corresponding to time instant t should be estimated and then substituted in equation (2.3) to determine sound field, $p(X,t)$ in the pipe. Equation (2.6) is nonlinear with respect to variable $\tau$ and is not amenable to being solved analytically. The numerical solution can be obtained by using MATLAB fzero function for very short time steps but it would be very computationally expensive. A mathematical trick was derived to feed fzero with initial values close to real solution of the equation. This idea helped fzero to converge faster and reduced computation time considerably.

If unknown variable "x" in the equation $f(x) = 0$ is considered where $f(x)$ is a continuous differentiable function, the solution of this equation is any value like "a" such that $f(a) = 0$ and $f(a-\xi) \times f(a+\xi) < 0$ where $\xi$ is a small number. Therefore we can say that the root of $f(x) = 0$ is the minimum of $abs(f(x))$ (shown by $|f(x)|$ hereafter) that meets $f(x) = 0$ condition as well (in other words, global minimum(ma) of $|f(x)|$ is(are) zero(s) of $f(x) = 0$ ). Hence, the zero-finding problem converts to minimum-searching one. The main characteristic of extreme points is abrupt change in slope of tangent line to $|f(x)|$ or in mathematical words

$$f'(x) = {df(x)}/{dx} \tag{2.7}$$

Mathematically, at discontinuity points of a function, taking derivatives is not identifiable (or the slope of the tangent line tends to infinity). So numerically, derivative values at discontinuities are very large numbers (peaks) in derivative graph. Consequently, finding zeros of $f(x) = 0$ would be transformed to locating peaks of the second derivative graph of $|f(x)|$. By finding the positions of those peaks we have solved the primary problem. But the story in discrete world is more challenging. "x" is an array of numbers with specific precision which is very determining in resulting to accurate solutions of equation $f(x) = 0$. In order to overcome numerical difficulties, the approximate solutions were estimated by following the mentioned procedure and then fed to MATLAB fzero function as initial values to obtain more precise solutions with smaller errors. This technique has been implemented in a MATLAB code. A brief description of whole procedure was depicted in a flowchart in the Figure 2.3. This algorithm is repeated for each time step and hence equation (2.6) is resolved for each time instant.

Results of simulation for a case where $f_p = 470Hz$, $f_c = 550Hz$, $A_p = 0.02m/s$ is shown in the following.

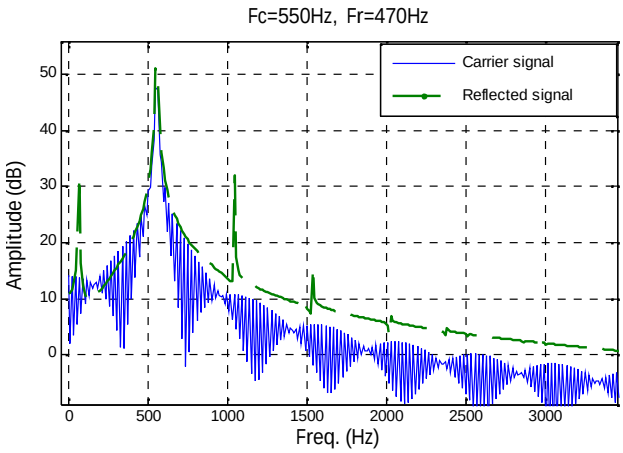


Figure 2.3: Simulation results for Doppler shift effect

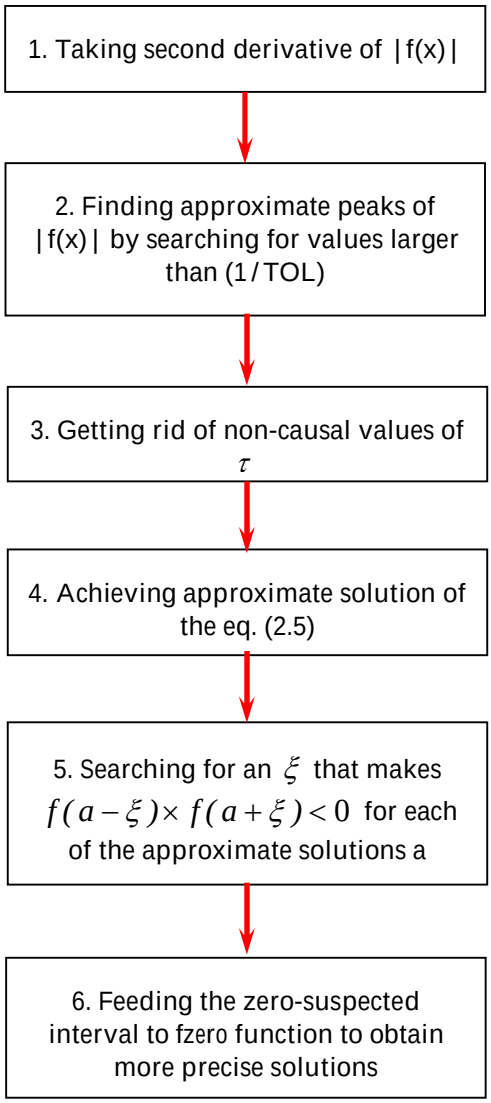


Figure 2.3: Simulation results for Doppler shift effect

# 3 Outdoor experiment

In order to experimentally verify the proposed technique for leak detection, an adequately long plastic pipe filled with water and pressurized up to 5bar was needed. A tank, pump and couple of valves were also necessary to build this indoor test rig. It was kind of hard to prepare these test facilities in the lab and therefore it was decided to use urban distribution network for trials. In one hand, it made life too hard by incorporating lots of unknown parameters like pipe material, exact dimensions, wave speed in the pipe and severe interfering background noise. On the other hand, it was an opportunity to evaluate this method in a real situation that it should cope with.

The experiment setup configuration and settings, trial site and recorded data are described in the following subsections.

## 3.1 Experiment setup

Experiment setup included the following components:

1. A connection tube to be mounted to access points, it makes a T-junction with the main pipe in the bottom end, in the other end it's equipped with adaptors for assembling transducers, shown in Figure 3.1
2. An emitter, it's made of a ceramic piezoelectric foil bonded to a steel membrane and wired to a BNC connector, depicted in Figure 3.2
3. A hydrophone, has a similar construction to emitter, made of a PVDF piezoelectric foil circuited with a built-in amplifier
4. Driving circuit of emitter, consists of U-shape transformer, a capacitor of high capacitance was connected in series to the input of transformer to protect signal generator as well as removing dc offset of input voltage (this constant dc value diminishes transformer performance)
5. Analogue signal generator, capable of generating trains of bursts with different interval time length
6. External amplifier to strengthen the signal measured by the hydrophone
7. Portable USB data acquisition device (DAQ)
8. Data logging software, A code was written in MATLAB to read measured signals from DAQ channels and store in a .mat file

Assembled test rig in the trial site was shown in Figure 3.3, Figure 3.4 and Figure 3.5. Table 3.1 presented more detail information about each of the components.

Figure 3.1: Test rig connected to the water pipe through a valve.

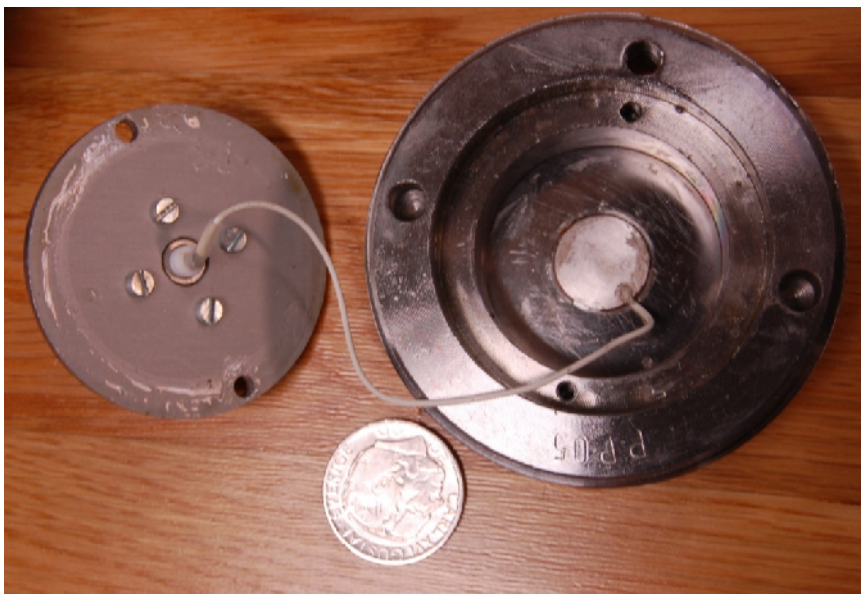

Figure 3.2: Emitter dismantled, 1 Kr coin demonstrates size of the PZT foil

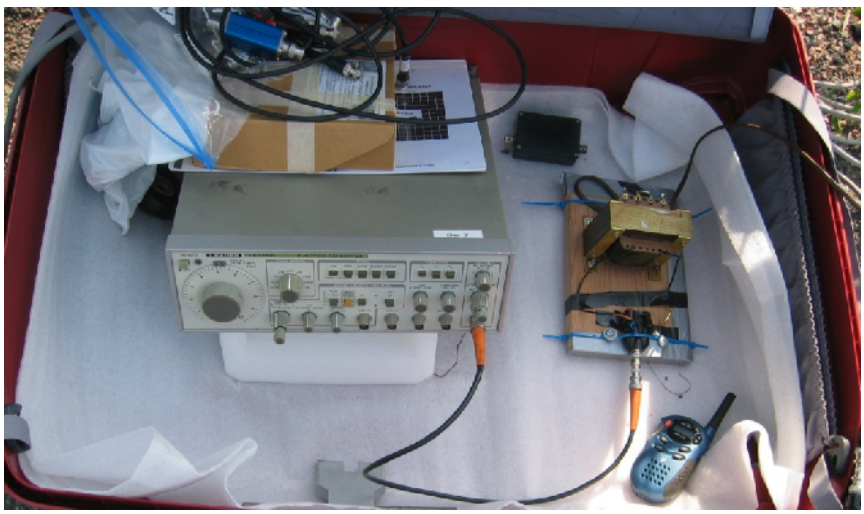

3

Figure 3.3: Signal generator and transformer, the output voltage from transformer drives emitter.

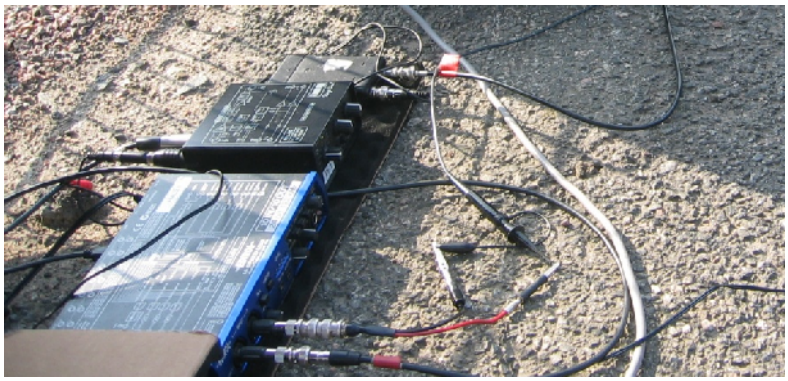

Figure 3.4: Portable USB DAQ and amplifier, the output voltage from hydrophone amplified and recorded.

Figure 3.5: The complete measurement setup in field trial.

Table 3.1 Experiment setup components

| Device | Description |
|---|---|
| Emitter | Handmade, ceramic foil probably PZ 26, Dia.= 16mm, Thickness = 1.1 mm, $C_0$ = 1.9nF, withstand 1000V / mm |
| Hydrophone | PVDF sensor with built in amplifier, output SNR 10:1, |
| Signal generator | LFG 1310, Leader electronics Co., output 20Vp-p |
| Transformer | Laminated core, Vout / Vin= 12 / 1, operates up to at least 1KHz without signal distortion |
| Amplifier | MPA-102, www.imgstageline.com, used gain 35dB |
| USB DAQ | EDIROL UA-101 audio capture, 24bit, 10Ch. In,10 Ch. Out, 2 analogue input channel used, sampling freq. 48Ksam / sec |

The transducers that have been used for experiments had already been hand-made for ULTRAC AB and delivered to us for measurements. The hydrophone including its built-in amplifier was accurate enough and worked linearly at frequency range of interest. On the contrary, the transmitter wasn't designed and created with this application in mind.

In general, because of the coupling between mechanical and electrical properties of ceramic material the force-velocity relationship and voltage-current relationship are tightly tied together. Therefore dynamic behaviour of ceramic material is determined by both mechanical stresses and electrical field [10]. The electrical properties of the ceramic is very frequency dependent, ceramic foil can be electronically modelled as a pure capacitor for low frequencies, below the first resonance frequency of the ceramic foil and as a combination of capacitor, resistor and inductor for frequencies close to first resonance frequency. There is similar analogy for modelling mechanical behaviour of ceramic foil. These two modelling together determine electromechanical behaviour of PZT transducer. Appropriate parameter selection will lead to a transducer design that can be derived easily while radiating sufficient acoustic power. If desired operating frequency range is lower than the resonance frequency of the transducer, because of capacitance characteristics of transducer, it would be difficult to optimally derive it from conventional linear amplifiers and some form of impedance matching network might be needed. We were interested in sending huge acoustic power in low frequency range (100-500Hz) but the emitter was not designed for this purpose. Its first resonance frequency was around 2KHz. Consequently, assembling appropriate drive circuit which can supply emitter with enough power was a big challenge for a while. To overcome this problem, several attempts were made and eventually we came up to an idea to add mass to the ceramic foil and consequently lowering its fundamental frequency. Hence, the original emitter was taken apart; a steel nut of about 50gr was then glued to the crystal and bonded to the steel membrane by conductive glue. An L-shaped holder arm screwed to the transducer ring to upraise BNC connector and provide more space for mass. The modified emitter was shown in the Figure 3.6. The new configuration set the first resonant frequency as low as about 550Hz which was acceptable.

A laminated core transformer levelled up output of signal generator by twelve times. The maximum drive voltage on emitter was almost 74 vrms (210v p-p). The customized emitter together with drive circuit could successfully radiate adequate acoustic power to the water pipe.

The external amplifier was used to boost sensed signal by hydrophone. Amplification gain set to 35 dB.

In the initial measurements the LeakFinder[2] instrument which was supplied from ULTRAC AB was used to record measured signals but due to its technical limitations for acquiring and saving data a multi channel portable

[2] For information about this device please see www.ultrac.se/eng/leakfinder.php

USB DAQ board was adopted instead. This DAQ device acquired analogue signals in two channels, channel one read output of amplifier (hydrophone measurement) and channel two logged reference wave signal picked up from the behind (BNC connector) of the transmitter. DAQ system was connected to a laptop and streamed digital readings via USB bus. DAQ board's drivers had already been installed in computer and defined in MATLAB. Each channel input could be monitored real time with the aid of MATLAB digital oscilloscope (Data Acquisition Toolbox). A code was written to save each channel reading in a mat file for future signal processing. Sampling rate during test was 24000 samples per second per channel (so corresponding knob in front panel of DAQ tool set to 48000 sample / sec )

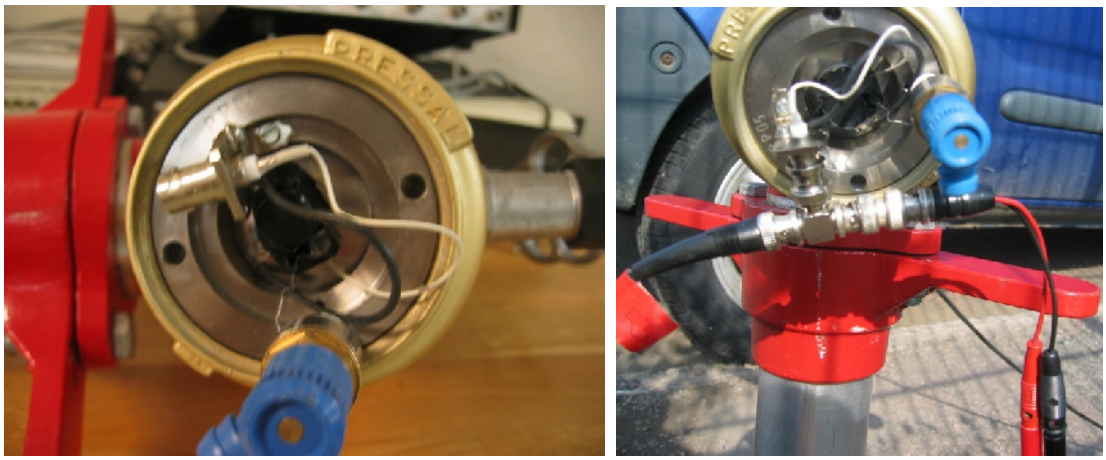

Figure 3.6: Close up of modified emitter.

## 3.2 The trial site

Part of urban water supply network at Stenkolsgatan, 417 07, Göteborg was used for measurements. Site and piping maps are shown in Figure 3.7and Figure 3.8. According to information received from Göteborg Vatten, the inspected water line was a buried 180PEH (Poly Ethylene High density) with a burial depth of almost 2m. Several attempts have been made to improve experiment setup and refine the weaknesses and shortcomings of the transmitter and DAQ devices from March 2010 to July 2010. The results presented in this report are based on the last attempt in a warm sunny afternoon from 3-6 PM on 29 June 2010. The air temperature was recorded to be almost 30 degree of centigrade. The experiment setup installed in the southernmost end of the pipeline, shown by a red S letter in the Figure 3.8, and a valve at 86m distance towards north was opened to simulate the leakage, its position shown by a red L letter in the Figure 3.8.

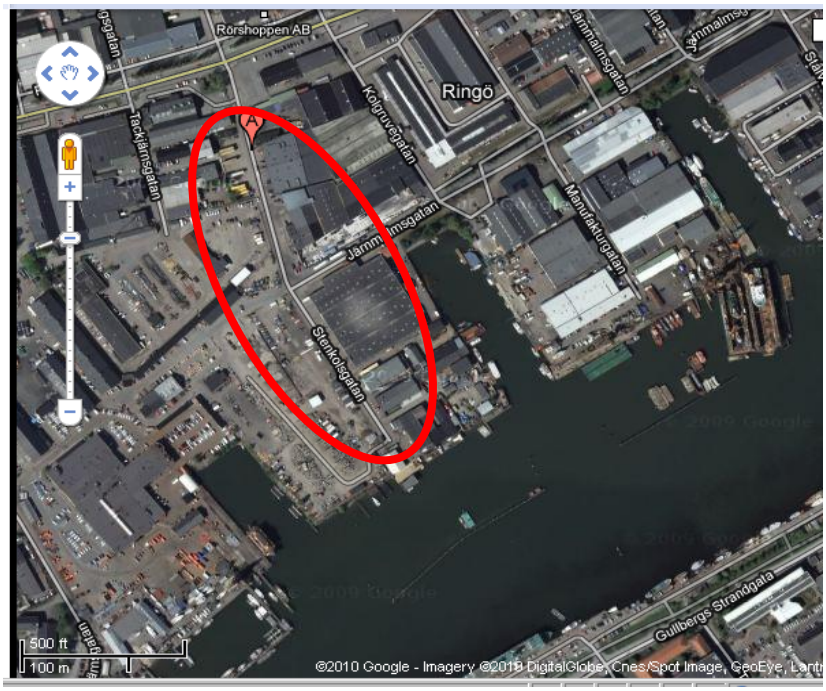


Figure 3.7: Site location specified by red ballon A, Stenkolsgatan, 417 07, Göteborg

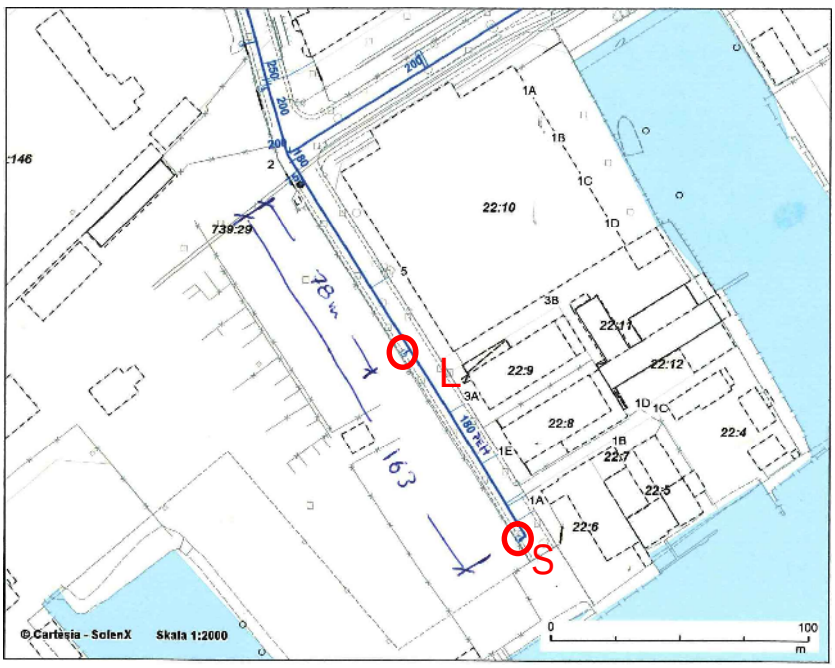


Figure 3.8: Piping map, thick blue line depicts inspected pipe, scale 1:2000, by courtesy of Cartesia

## 3.3 Recorded data description

As explained previously, the test procedure was to send a burst with known carrier frequency (Fc) and measure sound field in the pipe simultaneously for different pipe conditions. The experiments have been carried out with three different reference signals and at least in three conditions, they were:

- TRIAL 1; Fc=350Hz, Background noise (closed valve with no reference signal excitation), closed valve condition, closing valve condition, fully open valve condition and opening valve condition were measured, the burst was almost 1 sec long and time delay between consecutive bursts was 10 sec.
- TRIAL 2; Fc=400Hz, Background noise (closed valve with no reference signal excitation), closed valve condition, closing valve condition, fully open valve condition and opening valve condition were measured, the burst was almost 0.3 sec long and time delay between consecutive bursts was roughly 3 sec.
- TRIAL 3; Fc=550Hz, Background noise (closed valve with no reference signal excitation), closed valve condition, fully open valve condition and opening valve condition were measured. Additionally, the pipe response under only one burst cycle excitation was recorded as well. The burst was almost 0.3 sec long and time delay between consecutive bursts was 3 sec.

Recorded signals saved in arrays in MAT files. Arrays named such that included information about the test case (reference signal) and the test condition (valve state). For instance 'out400Hzopenvalve' refers to the case with Fc=400Hz as carrier frequency of the reference signal and the condition that a full leak does exist in the pipe (valve is fully open) at the location indicated by red L in the map (86m away). The first column of the matrix (array) assigned to channel one signal, i.e. hydrophone, and the second column contains channel two data, i.e. reference signal. This fashion respected for all measurements.

# 4 Signal processing

This was a challenging task to process the recorded signals in order to investigate existence of any reflection from the leakage and extract it if there was any while the wave speed in the pipe remained unknown. So the signal processing routine should be able to detect and distinguish the reflected signal from other intrusive noises in the time series. Since the essence of this new technique is that water leakage would distort the frequency contents of the reference signal Time-Frequency analysis of the signal would be the rational time series analysis technique among various available methods. Before moving forward to Time-Frequency analysis, the time representation of the signal as the first and most natural way of demonstrating physical systems were done in the first subsection. Then the frequency (spectral) representation of measured signals as a very powerful signal processing tool was carried out.

As an initial step in signal processing part, it should be noted that a measured signal represents an unknown physical process. The type of the process and as a result the signal is significant for choosing appropriate signal processing tools. According to the physics of the source and theory developed in the previous chapters it is expected that signals were originated from a partially deterministic process that contaminated with noise. Therefore it is sensible to classify this process in random process category with perhaps little degree of randomness. Respecting this categorization, the next step in signal processing would be to discuss on stationary condition of the signal. Generally speaking, in term of stationary property, a process, either random or deterministic, is divided in stationary (either in strict sense or wide sense) or non-stationary. A random process would be stationary if statistics of the process are invariant to a time shift and non-stationary processes otherwise. A signal is stationary in wide sense (WSS) if its mean and autocorrelation functions remain invariant with time shifts. These conditions for a time series x(t) can be expressed as:

$$\begin{aligned} &E(x(t)) = const. \\ &R_{xx}(t, t+\tau) = R_{xx}(\tau) \\ &\quad function \ \ only \ of \ \tau \end{aligned} \tag{4. 1}$$

Where $R_{xx}$ is the autocorrelation function and $\tau$ is an arbitrary time shift. These conditions verified for the recorded signals and approved that they are WSS signals. It gave us liberty to take advantage of a big number of available techniques for signal processing.

A deterministic signal is said to be deterministic if it can be decomposed to sum of sinusoids, i.e. as a sum of elements with constant instantaneous amplitude and frequency.

## 4.1 Time representation of signals

The time series of recorded signals for different reference waves and pipe conditions were depicted in the following figures. One cycle of system responses in different pipe conditions, likewise open valve and closed valve conditions, were split from the entire signal and shifted such that start from almost the same time instant. The region which was suspicious of containing reflections was magnified.

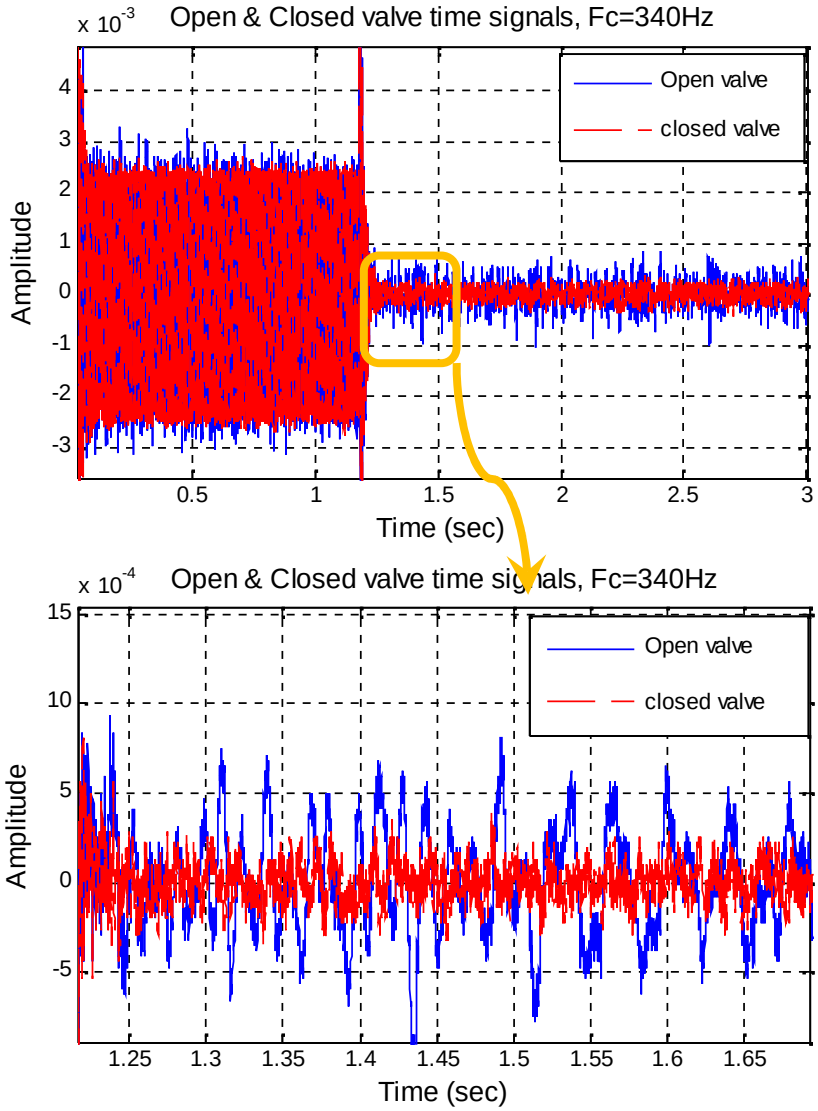


Figure 4.1: Time domain representation of measured signals for case 1, Fc=340Hz, open and closed valve conditions

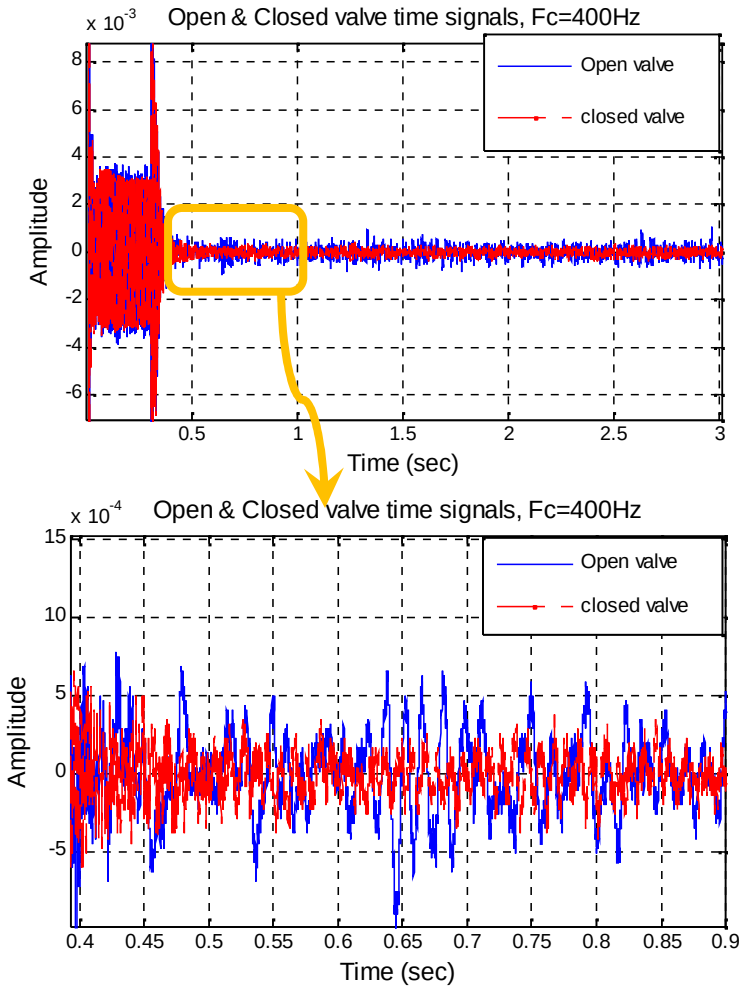


Figure 4 2: Time domain representation of measured signals for case 2, Fc=400Hz, open and closed valve conditions

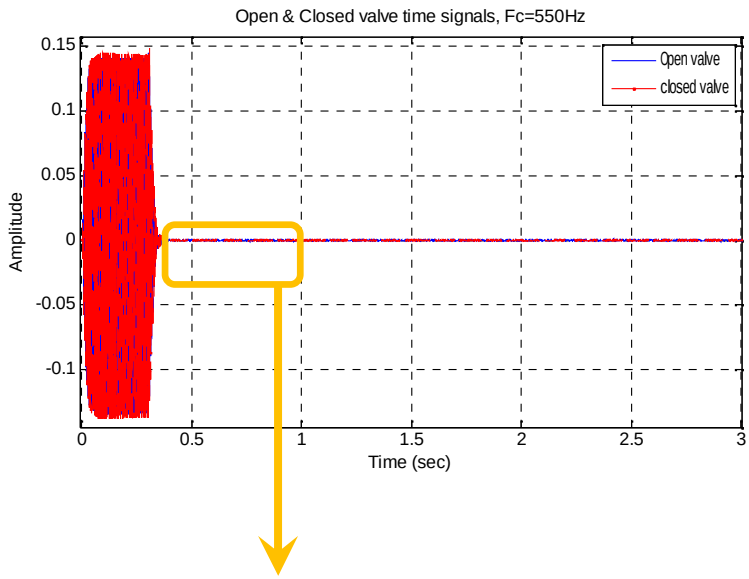

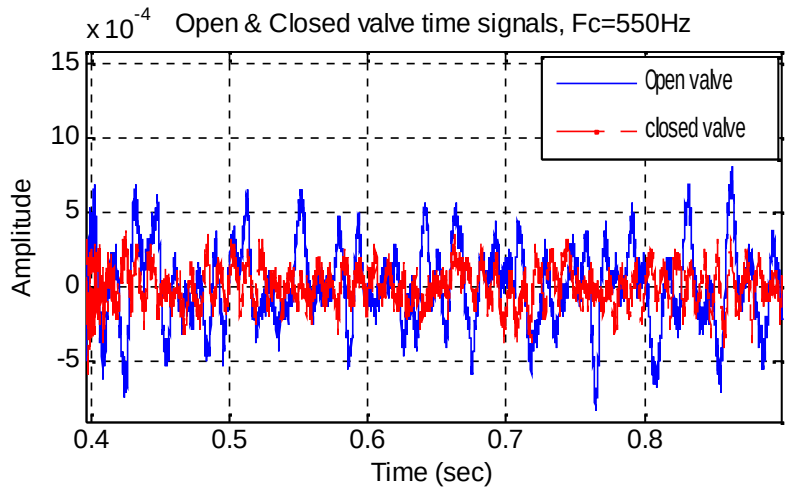


Figure 4 3: Time domain representation of measured signals for case 3, Fc=550Hz, open and closed valve conditions.

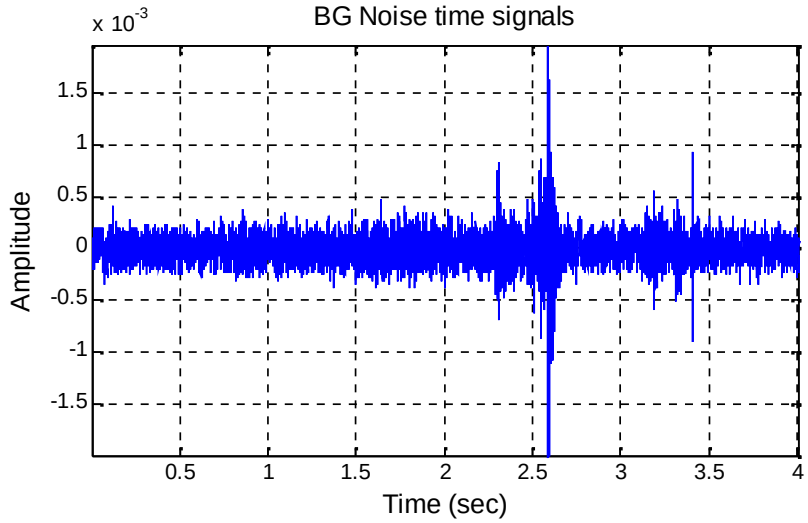


Figure 4 4: Time domain representation of measured background noise for case 3, Fc=550Hz.

Above figures show clear distinctions between open and closed valve states in all measurements. There is acoustic energy in the time series in open valve state after the main part of the burst dies out. This acoustic energy can be reflection of the burst already sent to the pipe or the noise generated from the leak due to sharp pressure drop close to the leak. It's almost impossible to distinguish these two by only looking at time plots however time graphs give a sense about possibly low frequency contents of the signal, e.g. by estimating peak-to-peak time intervals.

## 4.2 Frequency representation of signal

There are several ways to characterize a signal in the frequency domain. The mapping between time and frequency domains is done by Fourier transform. Mathematically it is expressed as,

$$X(f) = \int_{-\infty}^{\infty} x(t) e^{(-j2\pi ft)} dt \quad (4.2)$$

Fourier transform of a signal actually expands it to the family of infinite waves which are completely unlocalized in time. In the signal processing it is usually favourable to know the distribution of energy of the signal over frequency band, energy per hertz. Its called spectrum, power spectrum or power spectral density (PSD). The following theorem defines the PSD notion for random process.

### 4.2.1 The Wiener-Khintchine-Einstein Theorem

For a wide sense stationary (WSS) random process X(t) whose autocorrelation function is given by $R_{xx}(\tau)$, the PSD of the process is [11],

$$S_{xx}(f) = F(R_{xx}(\tau)) = \int_{-\infty}^{\infty} R_{xx}(\tau) e^{(-j2\pi f\tau)} d\tau \quad (4.3)$$

Where F() denotes Fourier transform. Therefore Fourier transform of autocorrelation function is the power spectral density of signal.

There are several parametric and nonparametric methods to derive PSD of a signal which extensively explained in signal processing texts. Two nonparametric estimates of PSD which have been employed in signal processing part of this project were described briefly in the following.

The first and maybe extensively used estimation is periodogram which is defined as squared magnitude of the discrete time Fourier transform of the samples. From mathematical point of view it's expressed as

$$\hat{S}_{xx} = \frac{|X(f)|^2}{f_s L} \quad (4.4)$$

Where L is the signal length and $f_s$ is sampling frequency.

Another intuitive estimation is to estimate the autocorrelation function and apply it in Equation (4. 3). Thus it is defined as

$$\hat{S}_{xx}(f) = \int_{-\infty}^{\infty} \hat{R}_{xx}(\tau) e^{(-j2\pi f\tau)} d\tau \quad (4.5)$$

The estimation of autocorrelation $\hat{R}_{xx}(\tau)$ can be derived from its definition. MATLAB function xcorr in unbiased estimation mode was utilized for this purpose. The advantage of using this approximation is that uncorrelated noise in the signal is cancelled out to some extent because of the convolution of signal over itself.

Spectra are sorted in two different ways namely 'trial by trial' and 'case by case'. In the case by case approach, three cases were defined namely BG noise

case, open valve case and closed valve case. The spectra of measured signals for the last trial (fc=550Hz) for different cases were plotted here, please refer to Appendix B for spectra of other trials and cases.

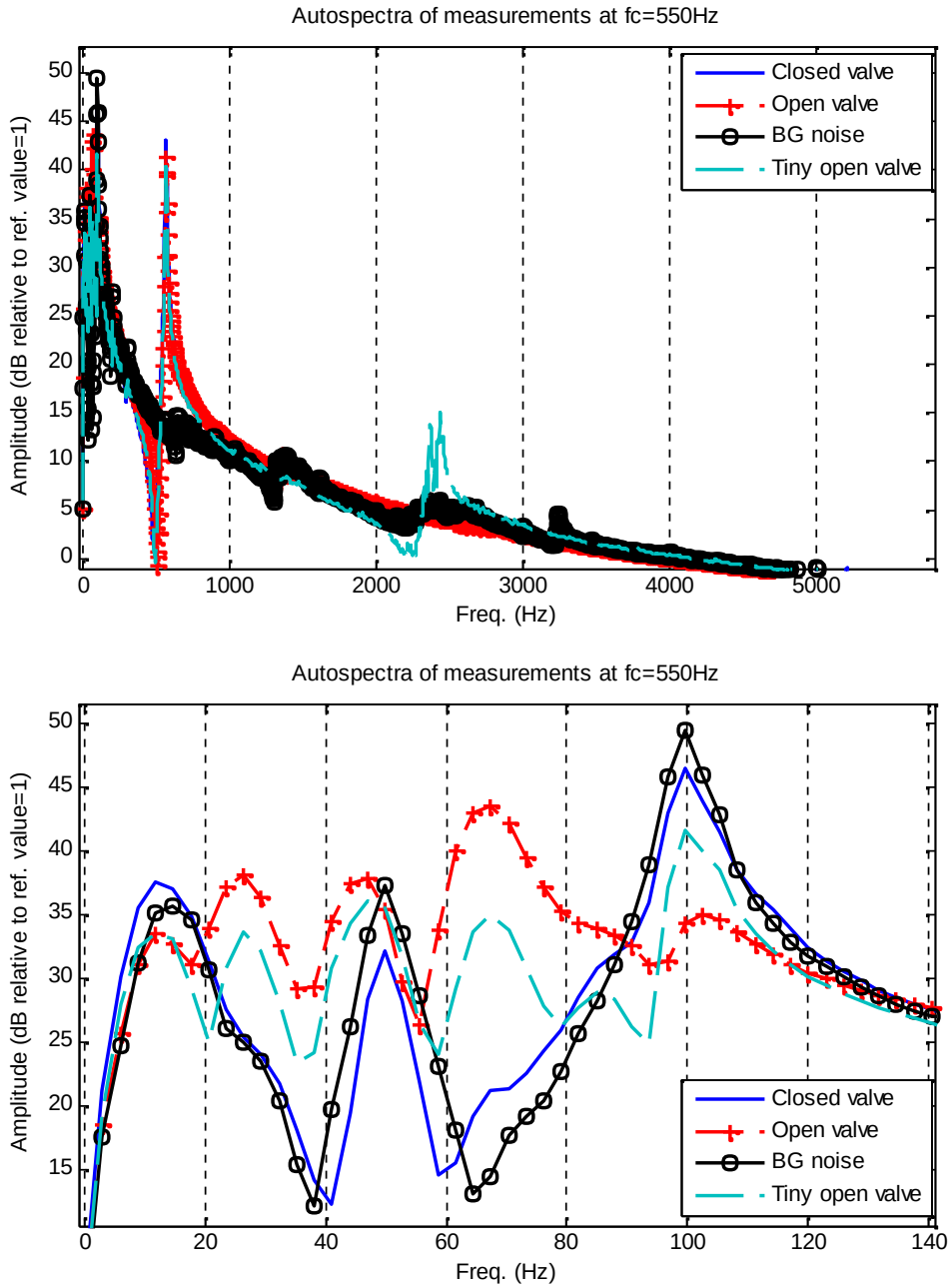


Figure 4.5: Spectra of signals of Trial 3 (fc=550Hz) for different cases, namely fully open valve, tiny open valve, closed valve and background noise

These spectra clearly show leakage makes new peaks while suppresses some others. The system (pipe) response to the change was roughly in the same fashion for all measurements.

Spectrum obviously explains what frequencies are contained in the signal, as well their corresponding amplitudes and phases, but does not say anything about the time instant these frequencies occur. In order to fulfil this demand the Time-Frequency analysis of signals were accomplished in the next section.

## 4.3 Time-Frequency analysis

Time-frequency analysis is a very important subject in signal processing. A lot of techniques have been developed in order to answer practical problems like radar signals, sonar, remote sensing and many others. The energy distribution method was utilized in this research.

In contrast to two approaches already mentioned, i.e. linear time and frequency representations, the aim of the energy distributions is to disperse the energy of the signal over the two description variables namely time and frequency simultaneously. Based on the periodogram definition, this can be written as

$$\hat{S}_x(t,f) = \left| \int_{-\infty}^{\infty} x(t)w(t)e^{(-j2\pi ft)}dt \right|^2 \quad (4.6)$$

Where $x(t)w(t)$ is windowed signal and $w(t)$ is window function. Several window functions are available for different signal processing purposes. Referring to Lampert [11] the common window for underwater remote sensing and sonar applications is Hamming that took in our application too. It's defined as

$$w(t) = 0.54 - 0.46\cos\left(\frac{2\pi t}{T}\right) \quad (4.7)$$

T is window time length (period). An alternative window which was examined and revealed good results was Gaussian window. It could also suppress side lobs and leak in STFT.

Relation (4. 6) can be interpreted as a joint time and frequency energy density. Hence point (t,f) in the spectrogram is a measure of energy density of signal at that particular coordinate which is usually visualized by the aid of colour spectrum. Eventually the following relationship summarizes this description about spectrogram energy distribution;

$$E_x = \int_{-\infty}^{\infty}\int_{-\infty}^{\infty} S_x(t,f)dtdf \quad (4.8)$$

$E_x$ the total energy of signal.

With regards to math point of view, Time-Frequency description of a signal is a quadratic map that transforms signal to jointed time and frequency domains. Properties of this mapping have been discussed in signal processing texts and were avoided to be repeated here but one significant characteristic of it should be recalled here. The spectrogram is the squared magnitude of the short FFT (STFT), therefore the time-frequency resolution of the spectrogram

is obviously limited exactly as it is for the STFT. There is a compromise between time resolution and frequency resolution. This poor resolution property is the main drawback of this representation and is not ignorable for our application. Frequency resolution should be fine enough to capture new harmonics associated to reflections from target that might arise in a particular time window.

The following formulas were used for discrete STFT in my code:

$$X(f) = \sum_{n=1}^{N} x(n)w(n)e^{(-j2\pi fn/N)} \tag{4. 9}$$

$$S(f) = \frac{|X(f)|^2}{\sum_{n=1}^{N}|w(n)|^2} \tag{4. 10}$$

W(n) is window function defined above.

Time-Frequency analysis was carried out for all measured signals; results for the last trial (fc=550Hz) were depicted in the following.

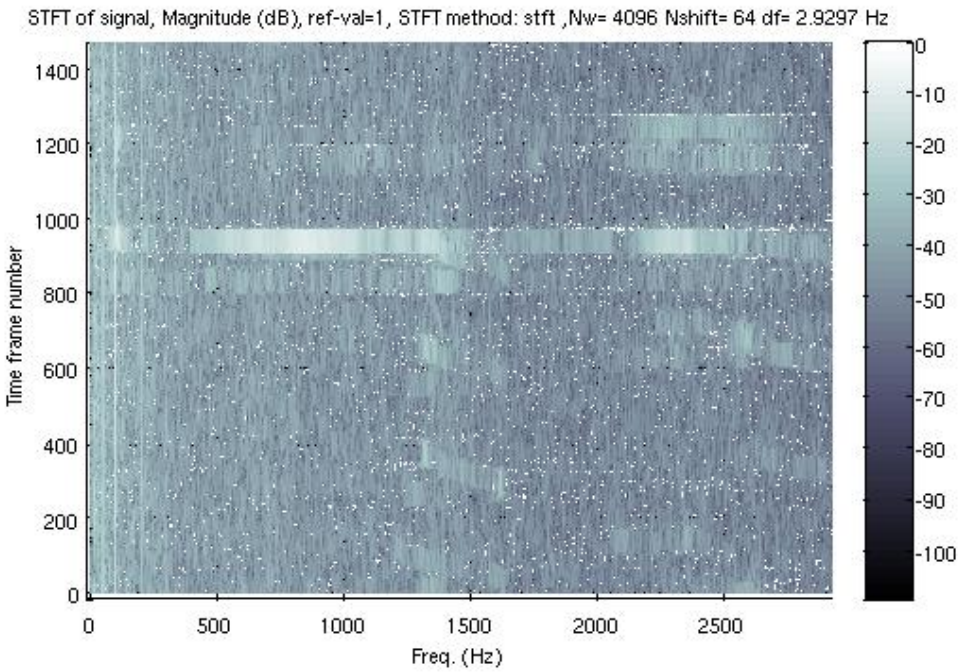


Figure 4.6: Spectrogram of background noise

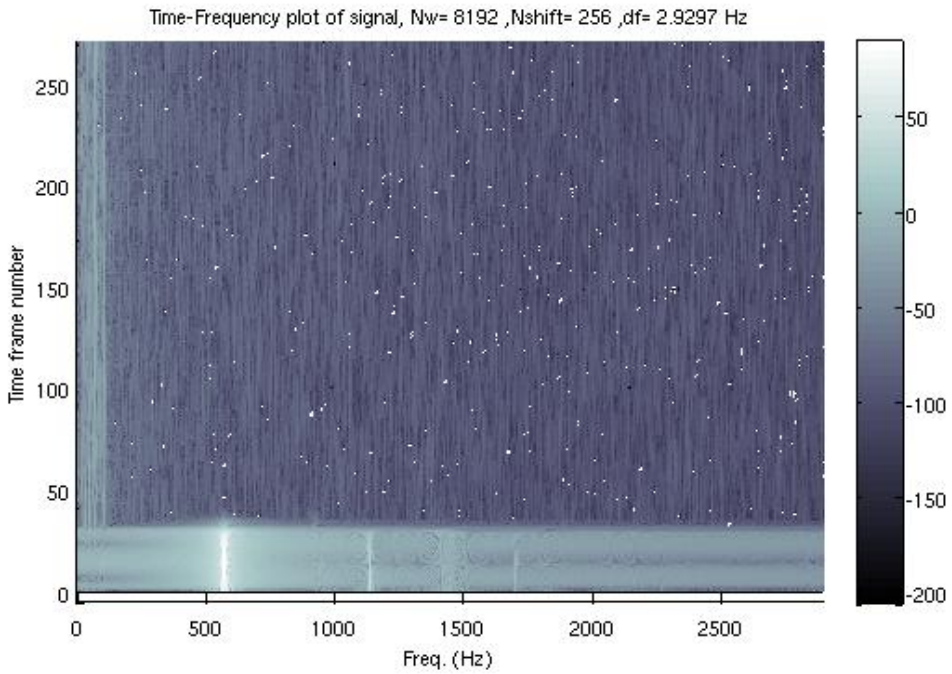


Figure 4.7: Spectrogram of open valve case, fc=550Hz

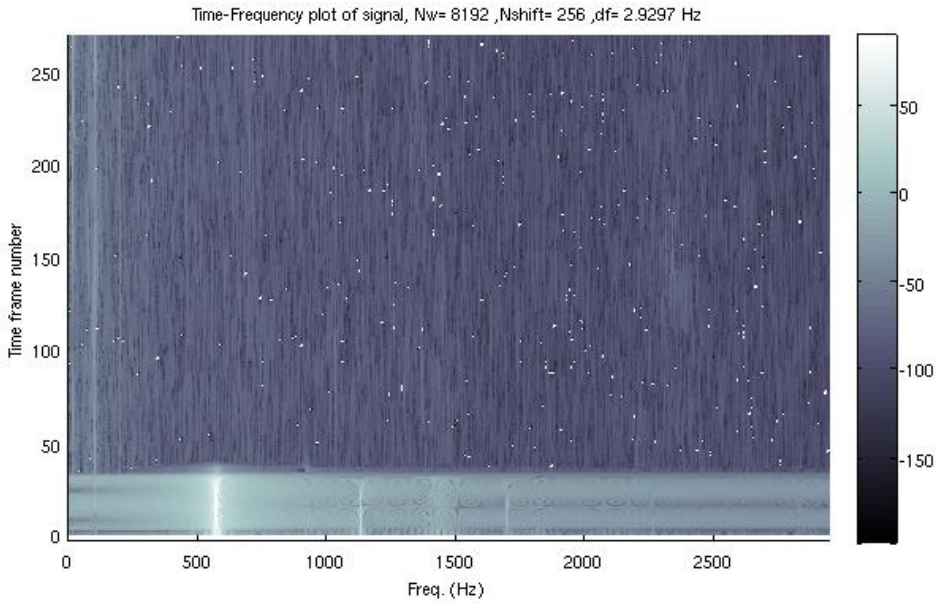


Figure 4.8: Spectrogram of closed valve case, fc=550Hz

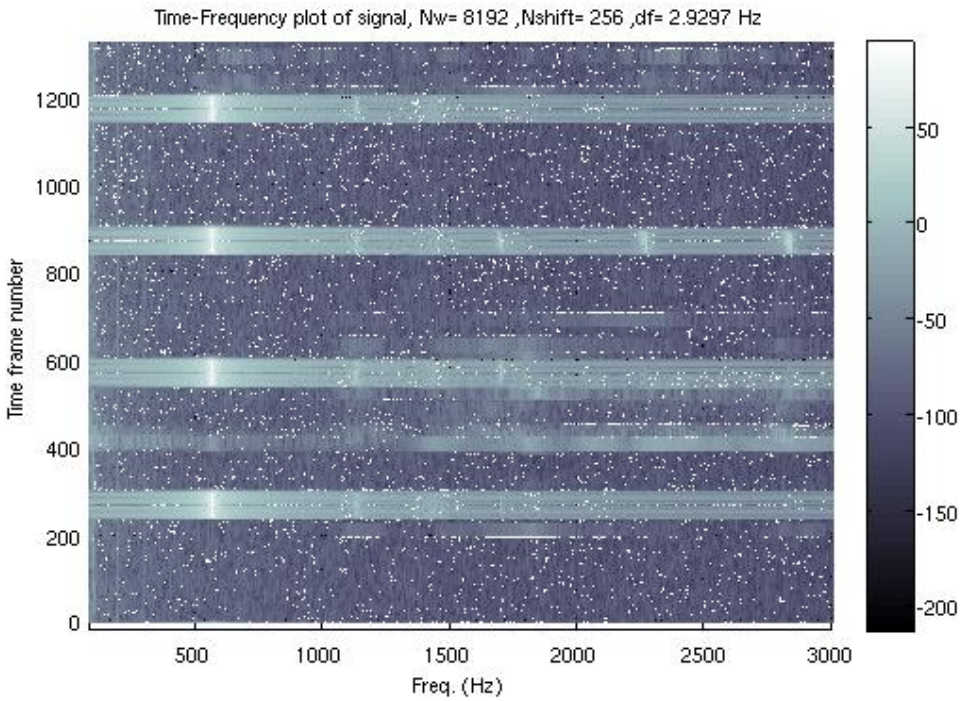


Figure 4.9: Spectrogram of opening valve case, fc=550Hz

In Figure 4.9 and Figure 4.12 pertinent to opening valve case, the spectrograms include pipe response to multiple bursts (four in Figure 4.9 and three in Figure 4.12) and therefore couple of reddish-yellowish stripes present in spectrograms.

## 4.4 Cross-spectrogram analysis

This name was chosen by me for this innovative technique. This is an idea that I came up with to process the leak signals in order to effectively overcome shortcomings of typical Time-Frequency analysis mentioned in preceding subsection. The main concept is to calculate cross-correlation between consecutive windows and then plot them in spectrogram. I can call it cross-spectrogram. As it was emphasized in the beginning of section 4.3 the spectrogram has a physical meaning, i.e. the energy is spread over time and frequency domains such that integration of spectrogram yields total energy of signal. In contrast to that, cross-spectrogram does not possess any physical meaning. It cannot be connected to energy distribution representation notion. Besides, cross-spectrogram takes advantage of cross-correlation definition which indicates the degree to which and fashion to two series are correlated. My idea was to investigate probable relationship between entries of two series of data; they are two subsequent windowed series. The DFT of sliding inner products of two time series were computed to see how frequent periodic similarities exist between series; it indirectly presents information about frequency contents of each time series as well.

Regarding math illustration, Equation (4. 5) was borrowed and modified in order to estimate cross-spectrum and mixed with Equation (4. 6) to take the

windowing effect into account, the final relation was obtained and used for calculations,

$$\hat{S}_{xy}(t,f)=\int_{-\infty}^{\infty} w(\tau)\hat{R}_{xy}(\tau)e^{(-j2\pi f\tau)}d\tau \tag{4.11}$$

$\hat{R}_{xy}(\tau)$ is estimation of cross-correlation between x(t) and y(t) time series. $w(\tau)$ are the Fourier coefficients of smoothing window. According to Ljung [13], for Hamming window $w(\tau)$ is

$$w(\tau)=0.5(1+cos(\pi\iota/\gamma)) \tag{4.12}$$

$\tau$ is time lag. Constant $\gamma$ controls window width.
This method unfortunately suffers from time and frequency resolutions trade-off too.
Cross-spectrogram analysis was carried out for all measurements, some results pertinent to Trial 3 were depicted in the following.

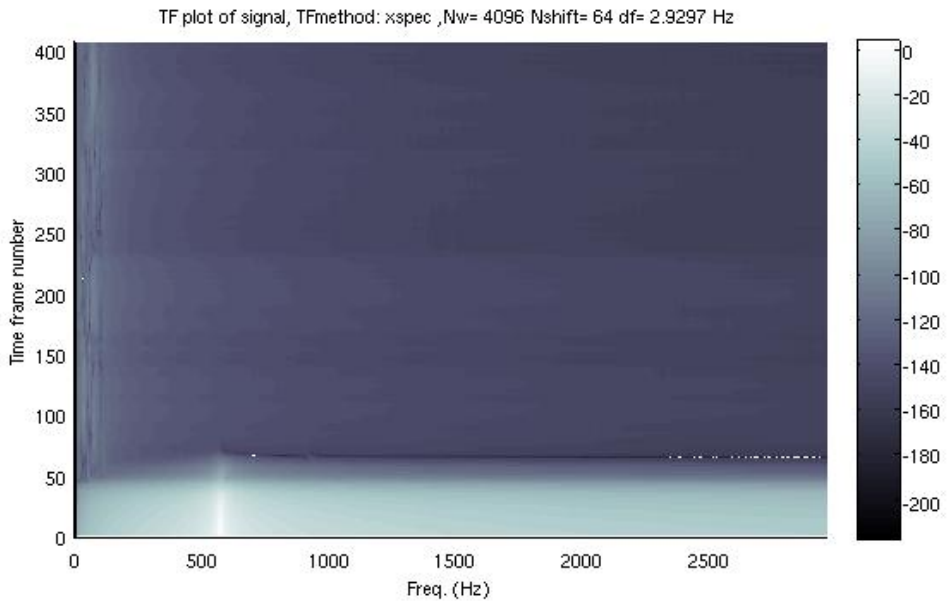


Figure 4.10: Cross-Spectrogram of open valve case, fc=550Hz

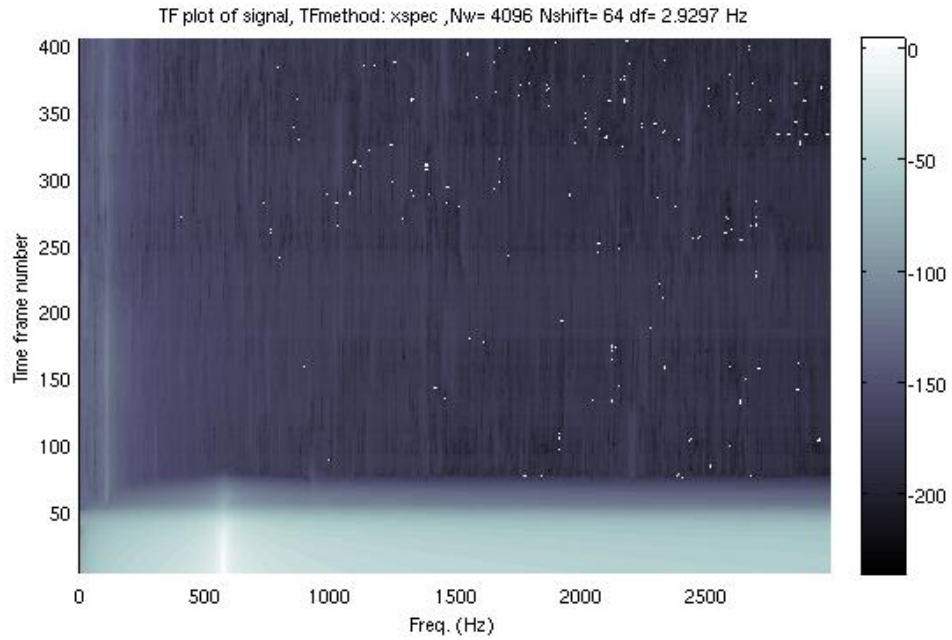


Figure 4.11: Cross-Spectrogram of closed valve case, fc=550Hz

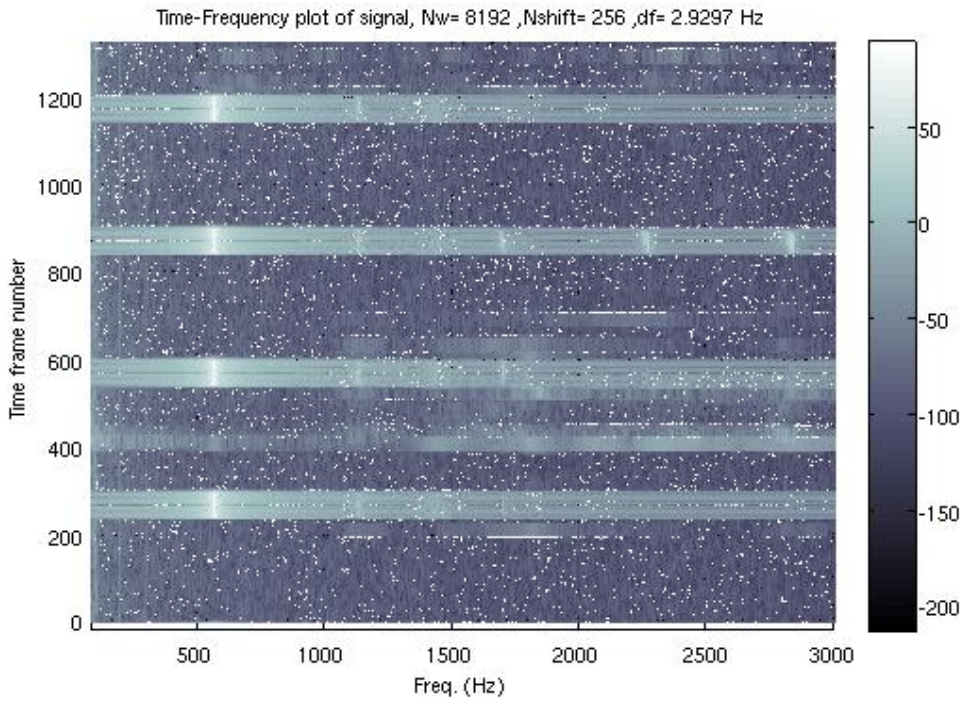


Figure 4.12: Cross-Spectrogram of opening valve case, fc=550Hz

It's truly difficult to compare these cross-spectrograms either with each other or with spectrograms shown in earlier section and deduce a pattern of changes in them. The necessity of exploring for spectrogram track detection techniques severely shows off, this topic researched and implemented in the next section.

## 4.5 Spectrogram track detection

The problem of discovering tracks in spectrogram has been investigated since mid of 1940s. Applications are plentiful and include identifying and tracking marine mammals via their calls, identifying ships, torpedoes or submarines via their radiated noise, meteor detection, speech format tracking and so forth. Several techniques have been addressed in literatures to deal with this problem; they can be loosely categorized as: image processing, neural networks and statistical approaches. A model from the last class of techniques was taken up and developed with the purpose of leak detection in mind.

Although the problem has been clarified in earlier section it would be helpful to go over it again here. In section 4.3 a visual representation of acoustic energy distribution across frequencies and over time was built up. In section 4.4 the interrelationship between succeeding windowed signals investigated and visualized in the same fashion. The aim is now to analyze these spectrograms to detect existing pattern of changes embedded in colourful spectrograms. The first step is to construct a matrix with the elements of spectrogram such that

$$\mathbf{S} = \left[S_{ij}\right]_{N\times M} = \begin{bmatrix} S_1(f_1) & S_1(f_2) & S_1(f_3) & \cdots & S_1(f_M) \\ S_2(f_1) & S_2(f_2) & S_2(f_3) & \cdots & S_2(f_M) \\ \vdots & \vdots & \vdots & \vdots & \vdots \\ S_N(f_1) & S_N(f_2) & S_N(f_3) & \cdots & S_N(f_M) \end{bmatrix}_{N\times M} \tag{4.13}$$

$S_{ij}$ is the value of either spectrogram or cross-spectrogram in i$^{th}$ window and j$^{th}$ element of frequency vector, equivalent to point (t,f) earlier discussed in section 4.3. N is the number of windows and M is the number of frequency elements.

Couple of Maximum Likelihood Estimators (MLE) were designed based on statistical assumptions regarding the data in question to decide whether a frequency bin contains noise or a track, i.e. acoustic energy. Rife and Boorstyn [14] suggests after calculating matrix S the maximum of the result is the MLE of the estimated frequency, $\hat{f}_i$, mathematically that is,

$$\hat{f}_i = arg\ \max_j \left[S_{ij}\right] \qquad i = 1,2,3,...,N \tag{4.14}$$

This MLE says that within each and every time frame i only a single frequency $\hat{f}_i$ which owns the maximum acoustic energy is selected to represent that time frame, the estimated track is therefore a series of these frequency positions. This MLE named as ‘method ‘1’’ in the written track detection MATLAB code and will be referred as MLE1 in this report. The outcome of applying this MLE on shown spectrograms and cross-spectrograms were depicted in the following.

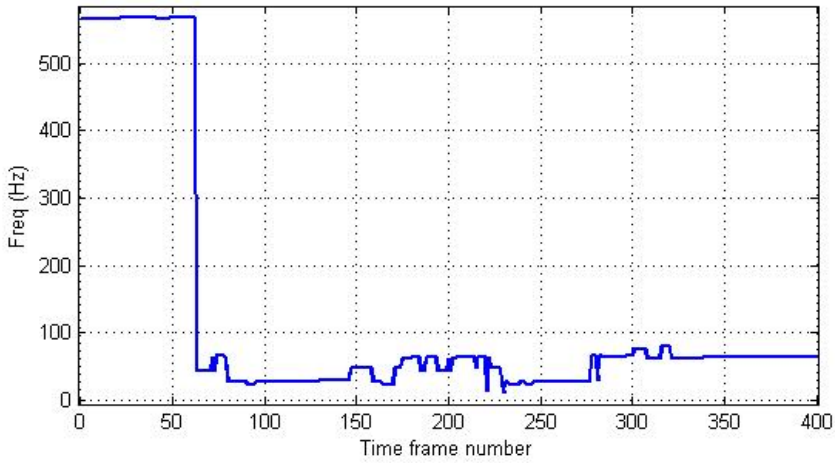


Figure 4.13: Detected track in Figure 4.7, spectrogram using MLE1, open valve case, fc=550Hz

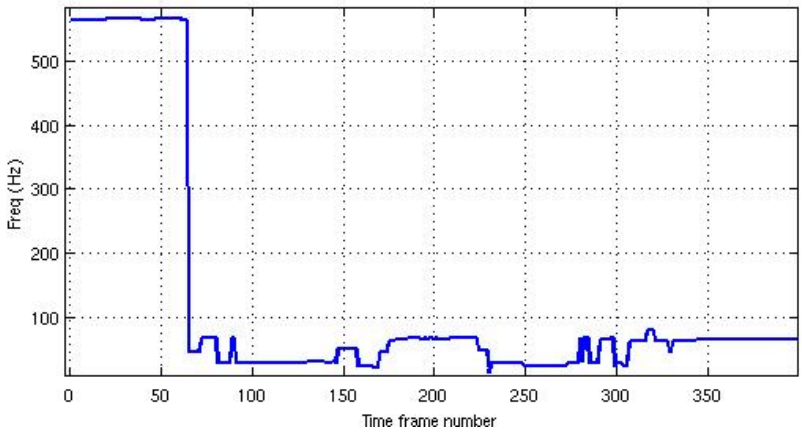


Figure 4.14: Detected track in Figure 4.10, Cross-spectrogram using MLE1, open valve case, fc=550Hz

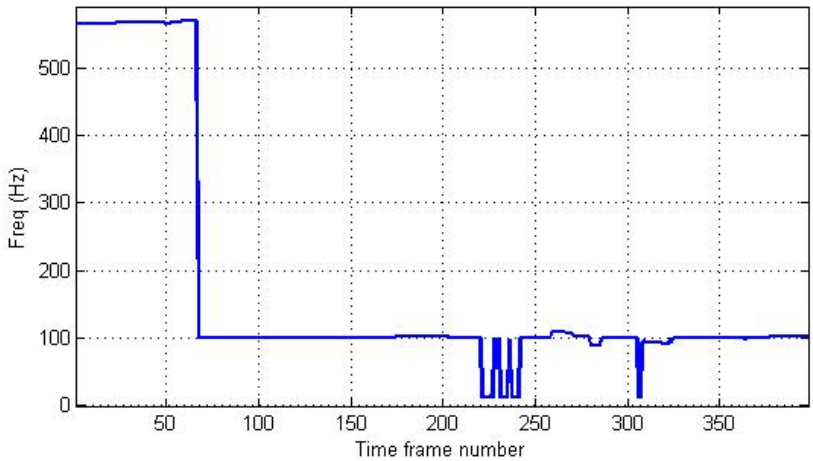


Figure 4.15: Detected track in Figure 4.8, spectrogram using MLE1, closed valve case, fc=550Hz

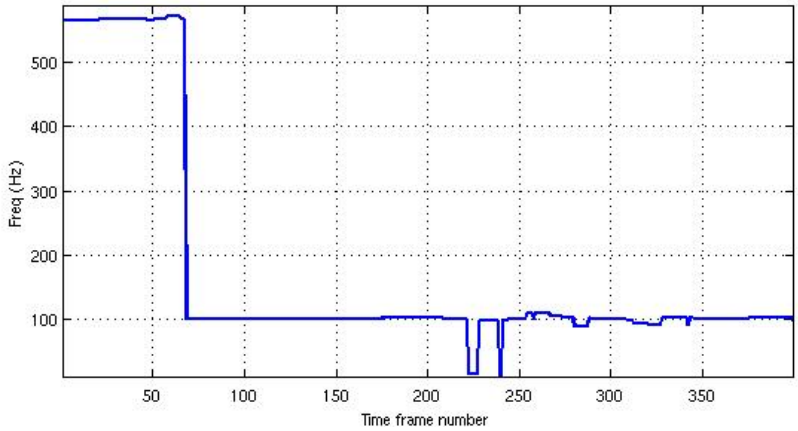


Figure 4.16: Detected track in Figure 4.11, Cross-spectrogram using MLE1, closed valve case, fc=550Hz

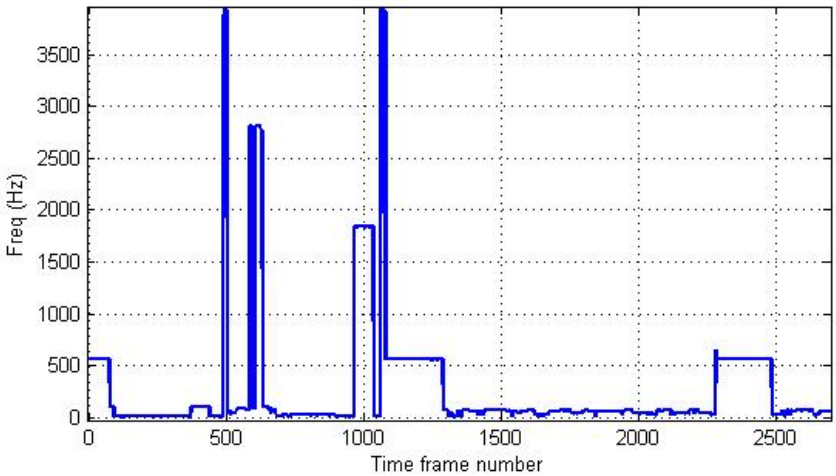


Figure 4.17: Detected track in Figure 4.9, spectrogram using MLE1, opening valve case, fc=550Hz

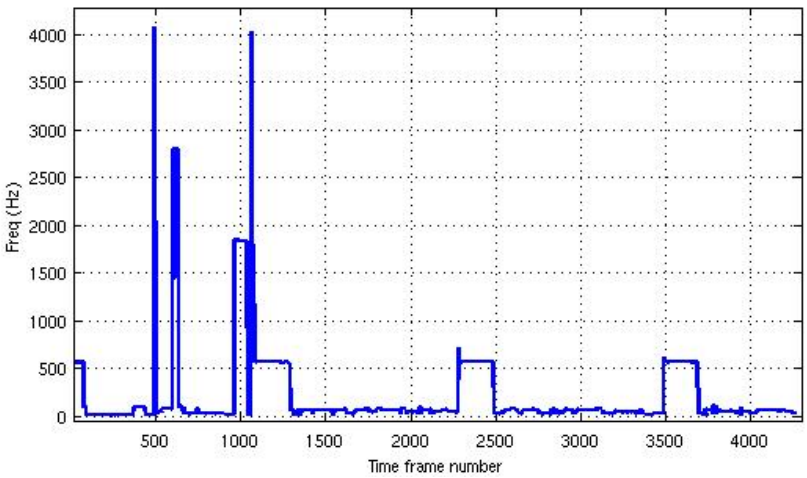


Figure 4.18: Detected track in Figure 4.12, Cross-spectrogram using MLE1, opening valve case, fc=550Hz

Since, change in (cross-)spectrogram due to received acoustic energy from leak is favorable, I thought it would be beneficial to look at the derivative of extracted pattern to put emphasize on variation between time frames, in other word;

$$diff(\hat{f}_i) = \frac{d\hat{f}_i}{di} \qquad i = 1,2,3,\ldots,N \tag{4.15}$$

Consequently, Figure 4.13 to Figure 4.18 are transformed to the following figures. They sorted case by case to facilitate comparison.

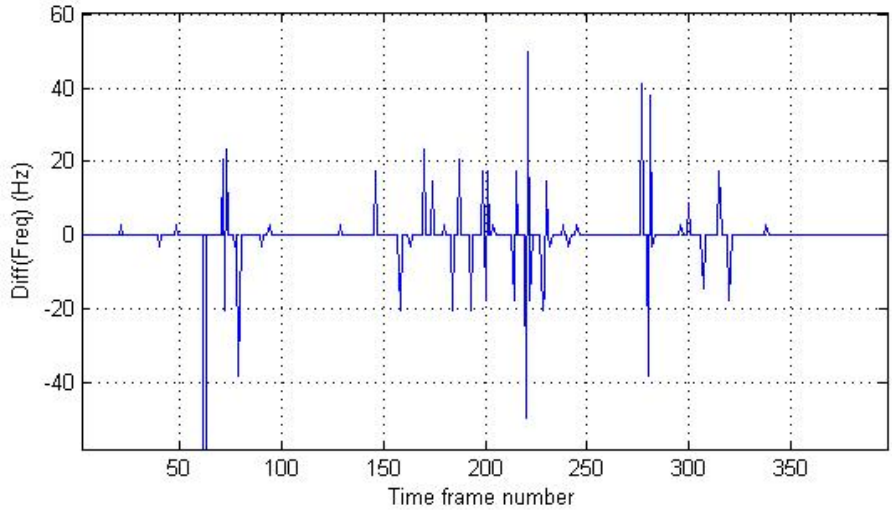


Figure 4.19: Derivative of Figure 4.13 with respect to time frame number, open valve case, fc=550Hz

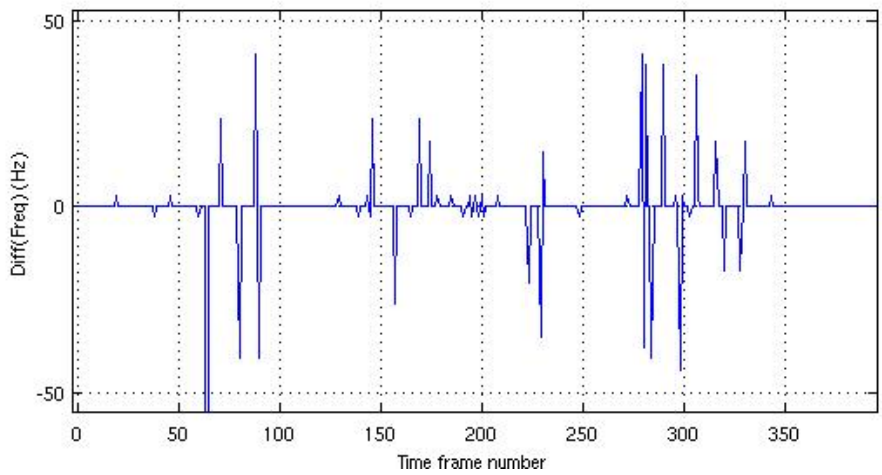


Figure 4.20: Derivative of Figure 4.14 with respect to time frame number, open valve case, fc=550Hz

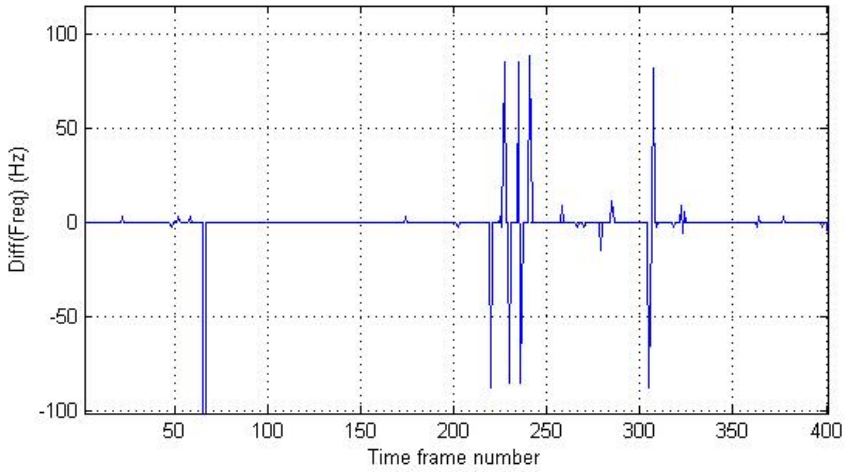


Figure 4.21: Derivative of Figure 4.15 with respect to time frame number, closed valve case, fc=550Hz

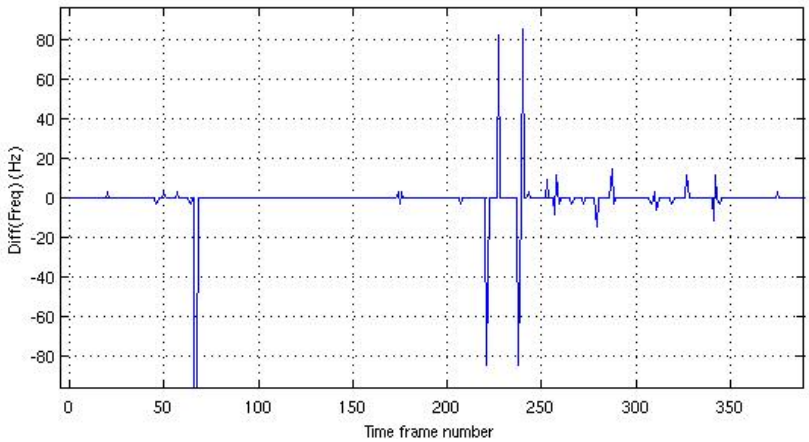


Figure 4.22: Derivative of Figure 4.16 with respect to time frame number, closed valve case, fc=550Hz

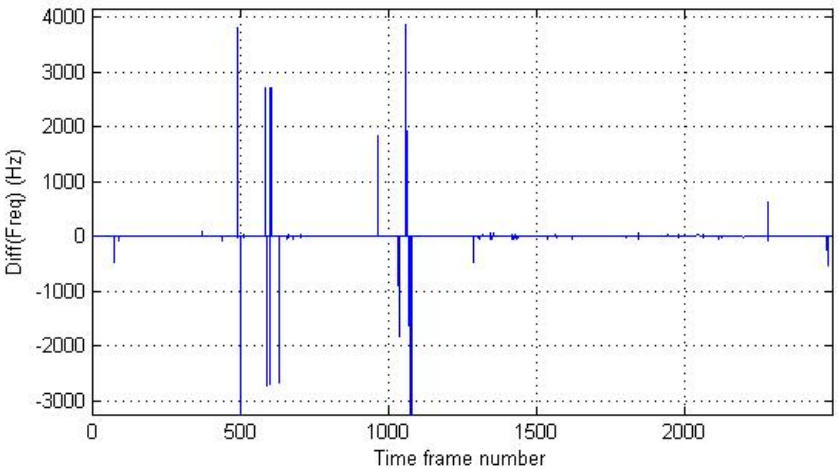


Figure 4.23: Derivative of Figure 4.17 with respect to time frame number, opening valve case, fc=550Hz

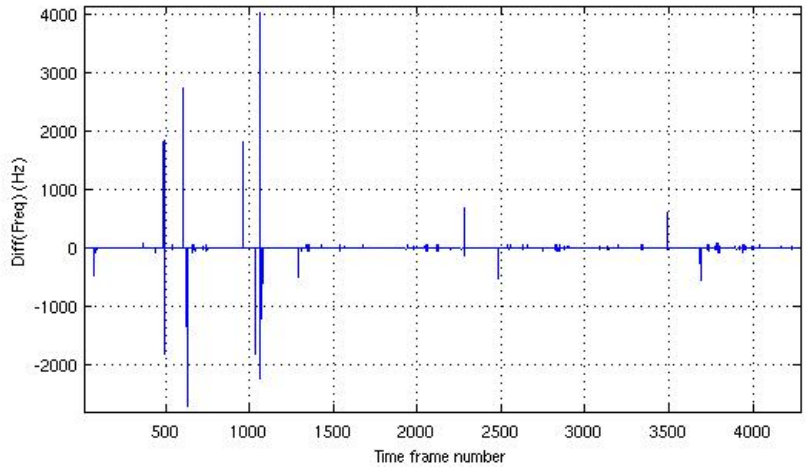


Figure 4.24: Derivative of Figure 4.18 with respect to time frame number, opening valve case, fc=550Hz

What if there were two or more frequency bins that gain from the equal amount of signal energy? The mentioned MLE is handicapped to detect track and more vitally the change may happen in track of (cross-)spectrogram. Barret and McMahon extended the above described MLE such that to find a fundamental frequency that its harmonics makes maximum contribution to total energy of signal at each time window. This multi-harmonic estimator is expressed as

$$\hat{f}_i = arg\ \max_j \sum_{k=1}^{m} \left| S_{i,kj} \right|^2 \qquad i = 1,2,3,\ldots,N \tag{4.16}$$

This new MLE was implemented; it is a very computationally expensive approach. Besides, as approaching to the end of frequency axis fewer number of frequency bins are accounted and therefore the estimated value becomes smaller and impairs its contribution to the overall summation. The simplest way to resolve this flaw is to normalize the summation to the number of frequency bins encountered each time, so I proposed the modified MLS as,

$$\hat{f}_i = arg\ \max_j \left( \sum_{k=1}^{m} \left| S_{i,kj} \right|^2 / m \right) \qquad i = 1,2,3,\ldots,N \tag{4.17}$$

This MLE named as ‘Method ‘2’’ in the MATLAB code. After tracing spectrum of leak signals frame by frame I got this idea that always in each frame there are only three or four frequencies that have the big portion of spectrum energy while their positions and magnitudes frequently vary. Consequently I thought that a MLE that collect three maximum frequencies of each time frame would be more powerful to monitor the uncovered pattern of spectrogram. This MLE is computationally very fast. The average of these frequency bins chose as representative frequency. Since we are only interested to capture the alteration point, this selection would be acceptable. This track

detector named as ‘method ‘3’’ in the code. These new MLE estimators (methods ‘2’ and ‘3’ of code) were applied to data already depicted in Figure 4.7to Figure 4.12, only the derivative results shown in the following figures. They sorted case by case to facilitate comparison.

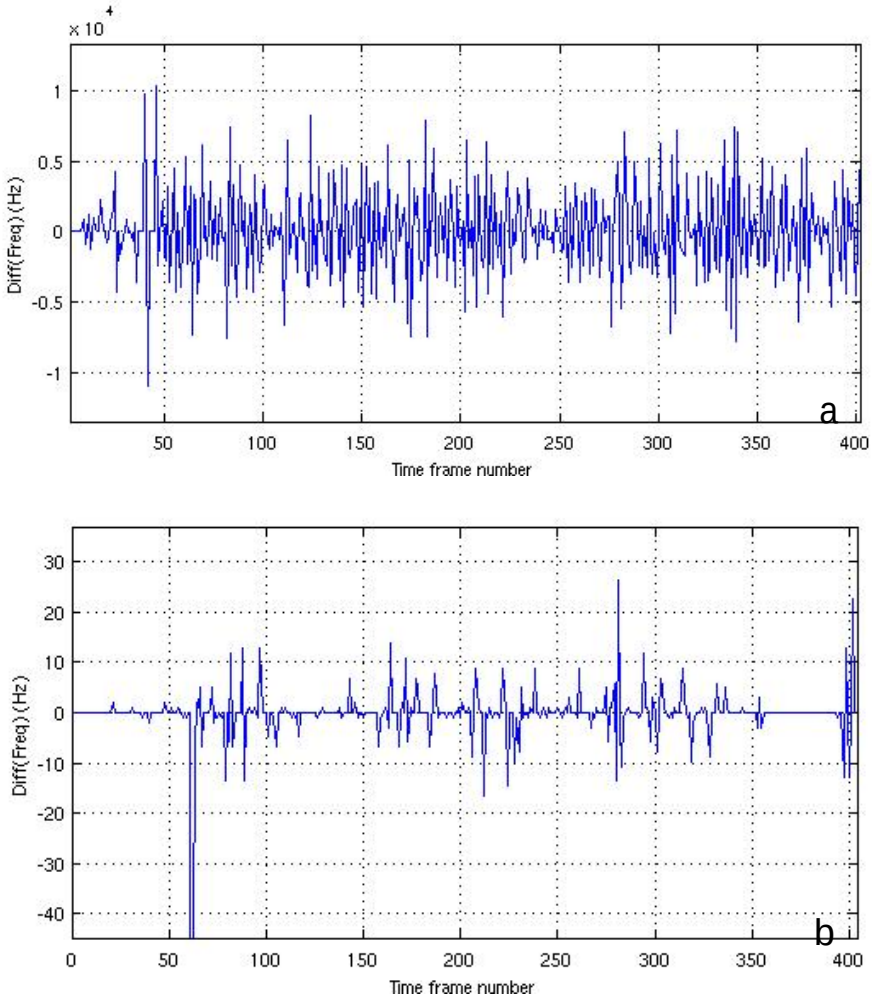


Figure 4.25: Derivative of detected patterns in Figure 4.7 using MLE of (a) method ‘2’,(b) ’3’, w.r.t to time frame number, open valve case, fc=550Hz

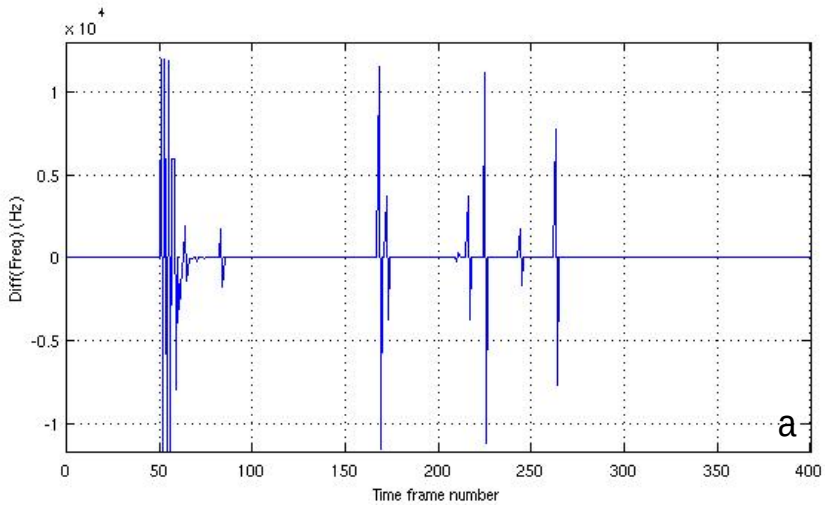

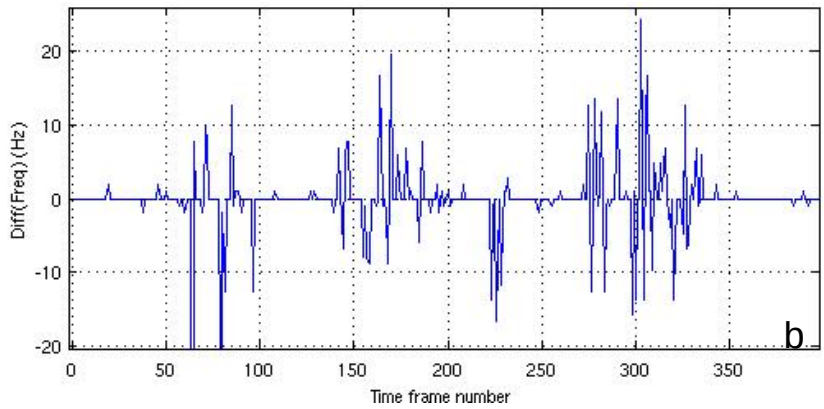


Figure 4.26: Derivative of detected patterns in Figure 4.10 using MLE of (a) method '2',(b) '3', w.r.t to time frame number, open valve case, fc=550Hz

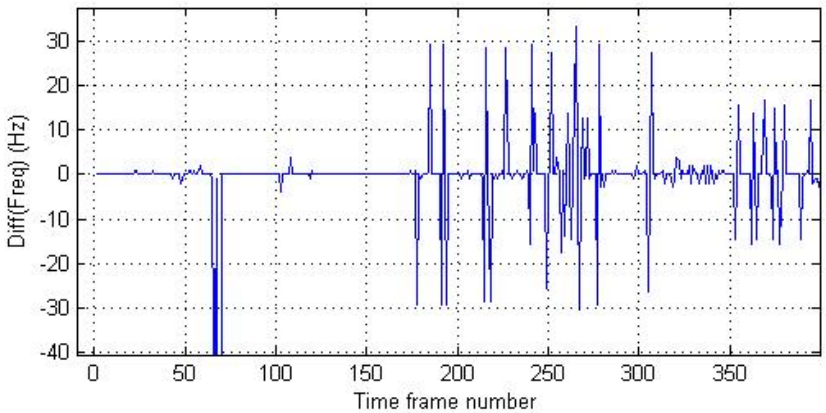


Figure 4.27: Derivative of detected patterns in Figure 4.8 using MLE of '3', w.r.t to time frame number, closed valve case, fc=550Hz

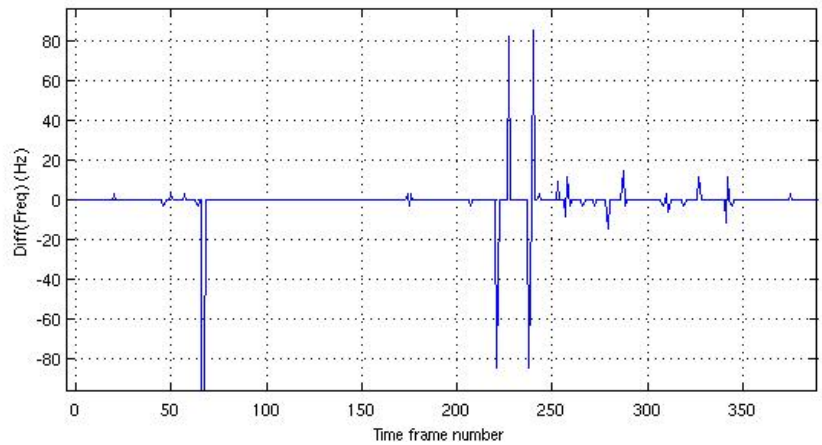


Figure 4.28: Derivative of detected patterns in Figure 4.11 using MLE of '3', w.r.t to time frame number, closed valve case, fc=550Hz

These difference plots are very useful in order to pinpoint leakage in the pipe. The discussion and summary of analysis was presented in the next section as the last chapter of this research report.

# 5 Discussion, conclusion and future work

The idea of pulse-echo analysis for leak detection was investigated in this research. A theoretical model for Doppler shift estimation from oscillating reflector; which is believed to be equivalent to physical model of leak, was developed. Doppler shift which occurs in this case is in form of generating new harmonics, in both low and high frequency ranges, rather than simple modulation in reference signal's frequency. Because of high attenuation in plastic pipes, mid and high frequency waves filtered out quickly. Therefore only low frequency contents of reflected waves can be measured in distances far away from leak location. Table 5.1 lists the frequency and magnitude of peaks in open valve case extracted from the spectra shown in section 4.2.

Table 5.1 Magnitude and frequency of peaks of spectra for open valve case, Mags. are in dB

| Open valve peaks (Hz) | 11.7 | 26.37 | 46.88 | 67.38 | 87.9 | 99.6 |
|---|---|---|---|---|---|---|
| Trial 1 (fc=340Hz) | 33.6 | 40.4 | 38.6 | 45 | 36 | 35.7 |
| Trial 2 (fc=400Hz) | 32.4 | 37 | 38.6 | 40 | 34 | 38 |
| Trial 3 (fc=550Hz) | 33.6 | 37.8 | 38.6 | 43 | ------- | 34.4 |

Since all these peaks arise in the same frequencies with more or less equal magnitudes, one can safely draw conclusion that these are related to the leak noise which was immutable during all open valve case measurements. In order to capture the right time instance that reflected reference acoustic energy arrives at the measurement point, time-frequency analysis was carried out using STFT and Cross-spectrogram techniques. The latter idea embarked and extended in this study with leak detection purpose in mind. Track detection algorithms were employed to serve us well in reading (cross-)spectrograms. Figures 4.15, 4.16, 4.21, 4.22 show that between time frames 200 and 250, a new tone with adequately big acoustic energy has been sensed. This behaviour repeated in some other closed valve trials and even open valve tests (but a little obscured). The only reason that I can deduce for this is reflection of reference signal from the T-junction discontinuity in 174m away from the test setup. This assumption leads to a guessed wave speed of 437 m/sec when fc=550Hz. Knowing the leak distance at about 85m distance, with respect to this guessed wave speed, it is expected to see a change in frequency content of spectrum at the time window of 68. Figures 4.13, 4.14, 4.19, 4.20, 4.25 and 4.26 show variation in energy (likelihood between successive windows) in frame number 71 which is in good agreement with the guessed one. So the peak at the time frame of 71 can be regarded as reflection of the signal from the leak. The results from MLE's when applied to cross-spectrograms are clearer and easier to interpret.

To summarize, It's shown that the pulse-echo approach can detect leak symptoms fairly well with the aid of high level signal processing techniques.

This technique cut the hardware expenses and measurement endeavours at the cost of high level signal processing efforts. As already mentioned, the working frequency range is very low, i.e. below 150Hz, therefore transmitter should be modified to be capable of generating sufficient acoustic power in low frequencies. Furthermore, successful application of this approach is tightly tied to the precise estimation of wave speed in the pipe.

Regarding further investigations, precise study of physics of leak phenomena is necessary to improve this technique reliability and performance. Additionally, influence of different parameters and situations like leak size, multiple leak situation, maximum operational distance and pipe size on performance of this technique should be studied. At the end, it seems this idea can work for localizing leaks in plastic water pipes however further researches should be carried out before its final implementations.

# 6 References

[1] Babbitt, H.E., The detection of leaks in underground pipes, Journal of AWWA vol. 7, pp 589-595, 1920.

[2] Andrew, F., Colombo, Lee, P., Karney, B., A selective literature review of transient-based leak detection methods, Journal of Hydro-environment Research 2, pp 212-227, 2009

[3] Inagaki, T., Okamoto, Y., Diagnosis of the leakage point on a structure surface using infrared thermography in near ambient conditions, NDT&E International, Vol. 30, No. 3, pp. 135-142, 1997

[4] Gao, Y., Brennan, M.J., Joseph, P.F., Muggleton, J.M., Hunaidi, O., A Model of the Correlation Function of Leak Noise in Buried Plastic Pipes, Journal of Sound and Vibration 277, pp 133–148, 2004

[5] Bimpas, M., Amditis, A., Uzunoglu, N., Detection of water leaks in supply pipes using continuous wave sensor operating at 2.45 GHz, Journal of Applied Geophysics, vol. 70, pp 226–236 , 2010.

[6] Gao, Y., Brennan, M.J., Joseph, P.F., Muggleton, J.M., Some Recent Research Results on the use of Acoustic Methods to Detect Water Leaks in Buried Plastic water Pipes, ISVR technical report, SO17 1BJ, 2009

[7] Muggletona, M., Brennana, M.J., Linford, P.W., Axisymmetric wave propagation in fluid-filled pipes: wavenumber measurements in in vacuo and buried pipes, Journal of Sound and Vibration 270, pp 171–190, 2004

[8] Muggletona, M., Brennana, M.J., Axisymmetric wave propagation in fluid-filled pipes: effects of wall discontinuities, Journal of Sound and Vibration 281, pp 849-867, 2005

[9] A.P. Dowling, J.F. Williams, " Sound and sources of sound "

[10] Kleiner, M., Electroacoustics and ultrasonics course compendium, http://www.ta.chalmers.se/education.php?page=cpg_eau

[11] Scott, M., Childers, D., Probability and random processes, Elsevier Inc., 2004

[12] Lampert, T.A., O'Keefe, S., A survey of spectrogram track detection algorithms, J. Of Applied Acoustics 71, pp 87-100, 2010

[13] Ljung, L., System Identification Theory for the User, 2nd Edition , Prentice hall, 1999

[14] Rife, D., Boorstyn, R., Single-tone parameter estimation from discrete time observations, IEEE Trans. Inform. Theory, 1974,20, pp 591-8

[15] Barrett, R., McMahon, D., ML estimation of the fundamental frequency of a harmonic series, Proceedings of ISSPA 87, Brisbane, Australia, 1987, pp 333-6

# Appendix A Table of wave speed in plastic pipes

V.11

**Polyethylene Pipe Velocity Values**

| DIA. | M.D.P.E. (PE80) SDR17.6 | M.D.P.E. (PE80) SDR11 | H.D.P.E. H.P.P.E. SDR17.6 | H.D.P.E. H.P.P.E. SDR11 | (PE100) SDR17.6 LOW - HIGH | | (PE100) SDR11 LOW - HIGH | |
|---|---|---|---|---|---|---|---|---|
| 16 | 357 | 391 | | | | | | |
| 20 | 315 | 346 | | | | | | |
| 25 | 280 | 307 | | | | | | |
| 32 | 264 | 283 | 290 | 310 | | | | |
| 50 | 227 | 280 | 249 | 307 | | | | |
| 63 | 226 | 278 | 249 | 305 | 236 | 274 | 302 | 350 |
| 90 | 221 | 260 | 243 | 286 | 237 | 276 | 301 | 350 |
| 110 | 204 | 260 | 224 | 286 | 236 | 275 | 302 | 350 |
| 125 | 203 | 261 | 223 | 286 | 236 | 275 | 302 | 350 |
| 160 | 203 | 261 | 224 | 286 | 236 | 274 | 302 | 350 |
| 180 | 203 | 260 | 223 | 286 | 236 | 275 | 301 | 350 |
| 200 | 204 | 260 | 224 | 286 | 236 | 275 | 302 | 350 |
| 225 | 203 | 260 | 224 | 286 | 236 | 275 | 302 | 350 |
| 250 | 203 | 260 | 223 | 285 | 236 | 275 | 301 | 349 |
| 280 | 203 | 260 | 223 | 285 | 236 | 275 | 302 | 350 |
| 315 | 203 | 260 | 224 | 285 | 236 | 275 | 302 | 350 |
| 355 | 203 | 260 | 223 | 286 | 236 | 274 | 301 | 350 |
| 400 | 203 | 260 | 223 | 286 | 236 | 274 | 301 | 350 |

**WARNING:** Polyethylene pipe velocity values vary considerably between manufacturers and can have variations between batches. Polyethylene pipes also vary with age and with conditions in service. A prolonged usage at higher pressures will result in a higher sound velocity. These figures have been calculated from manufacturers data, and apply to new pipe.

**FOR MAXIMUM ACCURACY OF RESULTS, YOU SHOULD PERFORM A VELOCITY MEASUREMENT ON SITE!**

# Appendix B Auto-spectra of other trials

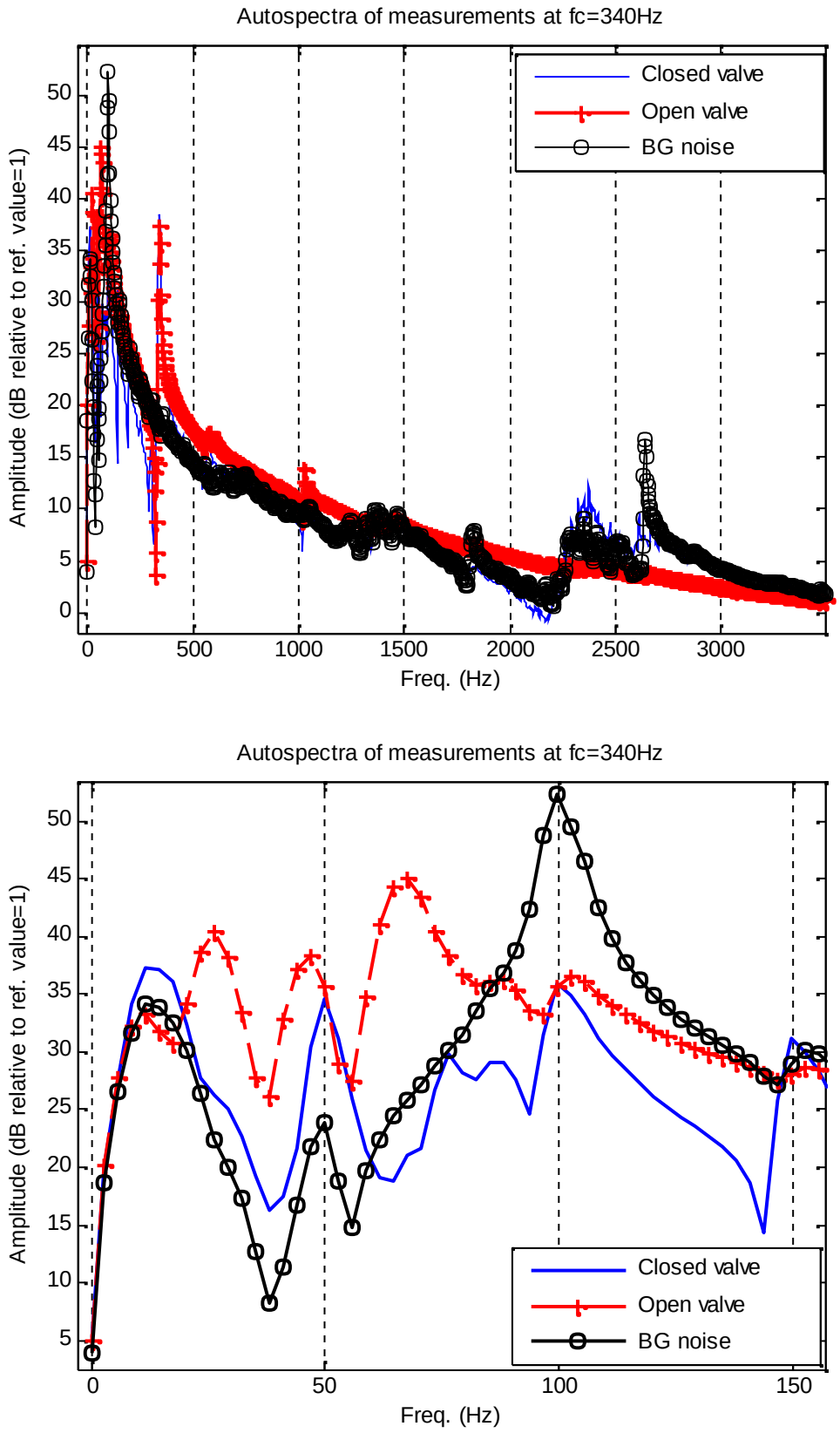


Figure B.1: Spectra of signals of Trial 1 (fc=340Hz) for different cases, namely fully open valve, closed valve and background noise

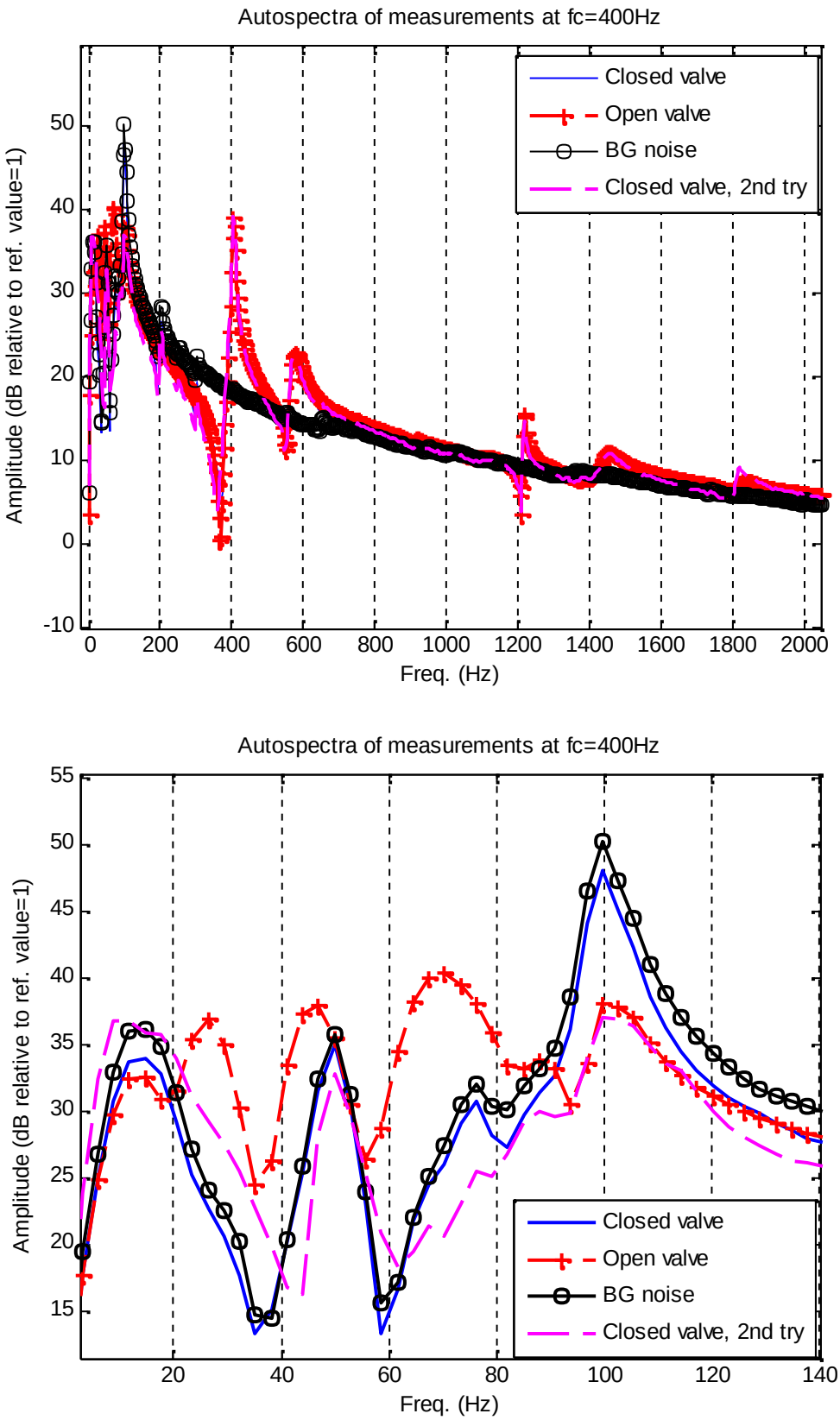


Figure B.2: Spectra of signals of Trial 2 (fc=400Hz) for different cases, namely fully open valve, closed valve and background noise